Chapter V: Provenance ages of the Neoproterozoix Katanga Supergroup (Central African Copperbelt), with implications for basin evolution[1]

S. Master[1*], C. Rainaud[1], R. A. Amstrong[2], D. Phillips[2,3] & L. J. Robb[1]

*([1]Economic Geology Research Institute-Hugh Allsopp Laboratory, School of Geosciences, University of the Witwatersrand, P. Bag 3, WITS 2050, Johannesburg, South Africa, *Sharadmaster@hotmail.com*
[2]PRISE, Research School of Earth Sciences, The Australian National University, Canberra, ACT 0200, Australia
[3]Present Address: School of Earth Sciences, University of Melbourne, Melbourne, VIC 3010, Australia)

Abstract: New age data on detrital zircons and micas are presented from key units within the Neoproterozoic Katanga Supergroup, which hosts the major stratiform Cu-Co deposits of the Central African Copperbelt. Detrital zircon ages indicate a mainly Palaeoproterozoic (between 2081 ± 28 to 1836 ± 26 Ma) provenance for the Katanga basin, derived from the Lufubu Metamorphic Complex of the Kafue Anticline and the Bangweulu Block to the north of the outcrop belt. Detrital zircons and clasts from the Grand Conglomerat glacial diamictite indicate a source from the Palaeoproterozoic metavolcanic porphyries and granitoids of Luina Dome region, which was a basement high during Nguba Group deposition. Minor zircons of Mesoproterozoic age may have been derived from the Kibaran belt. Finally, $^{40}Ar/^{39}Ar$ age data from detrital muscovites from Biano Group siltstones give a maximum age of sedimentation of 573 Ma, strongly supporting previous models that the Biano Group was deposited in a foreland basin of the Lufilian Orogen.

[1] *This paper will appear in Special issue Journal of African Earth Sciences, (Eds.) Robb, Cailteux, Sutton, in press.*

1. Introduction

The Neoproterozoic Katanga Supergroup is the host of the major stratiform sediment-hosted Cu-Co deposits, as well as numerous other deposits of Cu, Pb, Zn, U, Au, Fe etc., which constitute the Central African Copperbelt in Zambia and the Democratic Republic of Congo (D.R. Congo) (Robert, 1956; Mendelsohn, 1961a). In spite of its great economic significance there have been, up to now, few age data bearing on the deposition of the Katangan Sequence. We present here new SHRIMP U-Pb data on the ages of detrital zircons from Katangan sediments, as well as some preliminary ^{40}Ar-^{39}Ar data on detrital muscovites from the uppermost Katangan beds. These data give information on the age and likely nature of the source regions for the Katangan sediments and provide age constraints on upper Katangan (Biano Group) sedimentation (see Figure 1, Table 1).

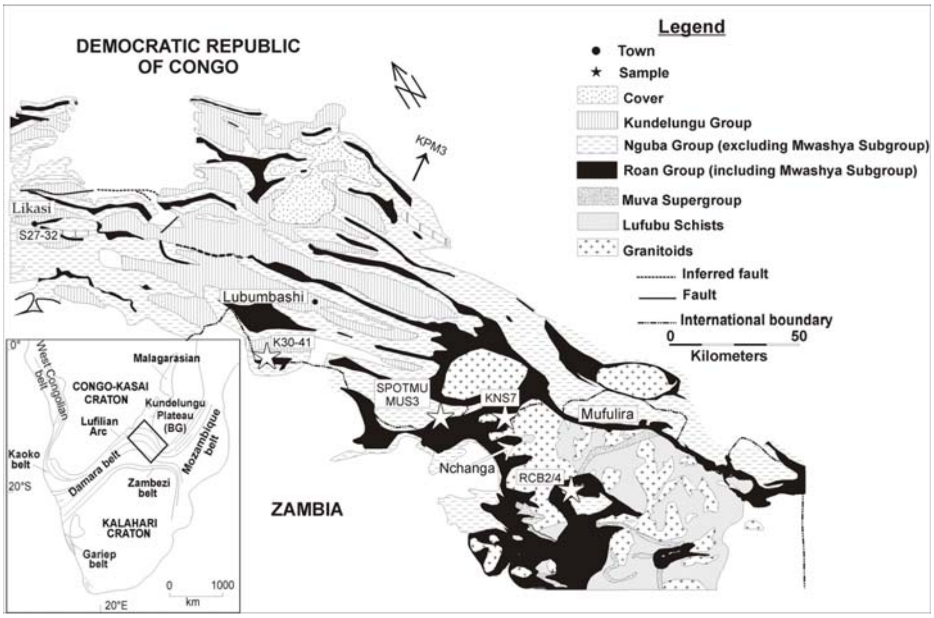

Figure 1. Simplified geological map of the eastern part of the Lufilian Arc in the Central African Copperbelt (after François, 1974), showing sample localities.

Katanga Supergroup

Group	Subgroup	Formation	Member
Biano			
Fungurume		Kambove	
		Dipeta	
		Musoshi	
Kundelungu	Kiubo		
	Kalule		
			Petit Conglomerat
Nguba	Monwezi		
	Muombe		
			Grand Conglomerat
	Mwashya		
Roan	Upper Roan		
	Lower Roan		

Table 1. Lithostratigraphy of the Katanga Supergroup (modified after Wendorff, 2003, and Cailteux, 2003).

2. Regional geological setting

In the Central African Copperbelt, the oldest pre-Katangan basement consists of a Palaeoproterozoic magmatic arc sequence, comprising the Lufubu Schists and intrusive granitoids, dated at between 1994 and 1873 Ma (Rainaud et al., 2004). Basement rocks are overlain unconformably by quartzitic and metapelitic metasedimentary rocks of the pre-Katangan Muva Group, which were deposited after 1941 Ma, based on the ages of detrital zircons (Rainaud et al., 2003). The Nchanga Granite is the youngest intrusion in the pre-Katangan basement (Garlick & Brummer, 1951; Garlick, 1973). It is an unfoliated coarse-grained peraluminous biotitic alkali granite with A-type geochemical characteristics (Tembo et al., 2000). SHRIMP U-Pb dating of zircons from the Nchanga Granite has yielded a concordant age of 877 ± 11 Ma, regarded as the age of the intrusion (Armstrong et al., 2004). The Nchanga Granite is nonconformably overlain by the Katangan sequence.

3. The Katanga Supergroup

The Katangan sequence consists of metasedimentary rocks traditionally divided into the Roan, Lower and Upper Kundelungu Supergroups (Cailteux et al., 1994; François, 1995). Current lithostratigraphic practice in the D. R. Congo is to subdivide the Katanga Supergroup into the Roan, Nguba (ex-Lower Kundelungu) and Kundelungu (ex-Upper Kundelungu) Groups, which are further subdivided into several subgroups (Cailteux, 2003). More recently, Wendorff (2001a,b; 2002a,b; 2003a) has proposed a new lithostratigraphic scheme, in which the Katanga Supergroup is subdivided into the Roan and Guba Groups, with two additional lithotectonic units, the Fungurume and Biano Groups, which he proposed were deposited syntectonically in a foreland basin during deformation of the earlier Katangan groups during the Pan-African Lufilian Orogeny. Wendorff (2003b) also uses the term “Kundelungu Group” to include the lower parts of the old “Upper Kundelungu” Supergroup, the Ks1 and Ks2 of Cailteux et al. (1995), which Wendorff (2003a) had included as the upper part of his “Guba Group”. In this paper, we adopt the lithostratigraphic scheme and terminology of Wendorff (2003b), except that we use the name “Nguba Group” instead of “Guba Group”, following the recommendations of Cailteux (2003), and existing practice among Katangan geologists. The lithostratigraphy of the Katanga Supergroup, as used in this paper, is summarised in Table 1.

a. Roan Group

The lowermost Roan Group of the Katanga Supergroup, subdivided into the mainly siliciclastic Lower Roan and the mainly dolomitic Upper Roan Subgroups (Table 1), consists of conglomerates, quartzites, arkoses, shales, siltstones, dolomitic shales, and anhydrite-bearing dolostones. The Roan Group is overlain unconformably by the Mwashya Subgroup, which forms the base of the Nguba Group.

Conglomeratic and arkosic sedimentary rocks at the base of the Lower Roan Subgroup of the Roan Group at Nchanga Mine nonconformably overlie the Nchanga Granite. Previous petrographic studies have indicated that there are pebbles and zircons from the Nchanga Granite in basal Roan conglomerates, suggesting that the lower Roan sediments are derived by erosion of a basement that included the Nchanga Granite (Garlick & Brummer, 1951; Binda, 1972; Garlick, 1973). A suite of detrital zircons from a cross-bedded Roan arkose above the contact with the Nchanga Granite, was extracted and dated by Armstrong et al. (2004). U-Pb SHRIMP dating of these detrital zircons reveals two distinct age populations, one at around 2.0 to 1.8 Ga (corresponding to the age of the Palaeoproterozoic basement), and the other at 880 Ma (corresponding to the age of the Nchanga Granite) (Armstrong et al., 2004). This unequivocally proves that the Nchanga Granite provided detritus to the Lower Roan, and sets a firm upper limit of c. 880 Ma for the age of the Katanga Supergroup.

The Upper Roan Subgroup is dominated by chemically precipitated and clastically reworked (mainly dolomitic) carbonate rocks and evaporites (anhydrite and gypsum), with few siliciclastic rocks. The depositional age of these rocks is poorly constrained except that they are intruded by numerous metagabbroic sills and dykes, which have given an age of c. 750 Ma (Armstrong et al., 2004). Hence that is a minimum age for the Upper Roan Group. At the base of the Upper Roan Subgroup, the Ore Shale Member (which hosts most of the mineralization in the Zambian Copperbelt) is cut by microcline-bearing metamorphic veins, which were dated from two localities- Roan Antelope Mine (now Luanshya, Zambia) and Musoshi Mine in D.R. Congo – using the Rb-Sr dating technique (Cahen et al., 1970). The two results taken together were interpreted by Cahen et al. (1984) to give a minimum age for the Roan Group of 870 ± 42 Ma. If the Rb-Sr ages of the microcline veins are accepted, then the age limits for the Roan Group are as follows:- Lower Roan Subgroup: maximum age c. 880 Ma; minimum age

870-42 = 838 Ma; Upper Roan Subgroup: maximum age c. 880 Ma; minimum age c. 750 Ma. If the Rb-Sr ages of the microcline veins are regarded as unreliable, then the Roan Group was deposited sometime between c. 880 Ma and c. 750 Ma.

b. Nguba Group- Mwashya Subgroup

The Mwashya Subgroup, formerly regarded as forming the top of the Roan Group (e.g., Cailteux et al., 2003), is now regarded as the lowermost subgroup of the Nguba Group, since it rests with an erosional unconformity on upper Roan Group rocks, as well as on older basement, and passes conformably into the Grand Conglomerat in places (Cahen, 1978; Wendorff, 2003b). It consists mainly of carbonates and black shales, but contains a thin pyroclastic unit with associated stratiform banded magnetite/haematite iron formations, which form a regional stratigraphic marker (Lefebvre, 1973, 1975; Cailteux et al., 2003a).

In western Zambia, in the Mwinilunga area, Key and Banda (2000) have mapped a several hundred metres thick volcanic unit within the Mwashya Subgroup, the Lwavu Formation, which consists of basalts and basaltic andesites. These volcanics have been dated at 760 ± 5 Ma, utilising SHRIMP U-Pb dating on zircons (Armstrong, 2000; Liyungu et al., 2001; Key et al., 2001). This is the first accurate date for any Katangan lithological unit. Recent dating by Barron et al. (2003) of two gabbroic bodies in the Solwezi area, NW Zambia, yielded ages of 745 ± 7.8 Ma and 752.6 ± 8.6 Ma, which are consistent with them being part of the extensional mafic magmatism associated with the Mwashya Subgroup (Kabengele et al., 2003).

c. Nguba Group- Grand Conglomerat Formation

The diamictite of the Grand Conglomerat has long been known to be a glacial tillite (Cahen, 1978). The evidence for a glacial origin of this diamictite rests on the common and widespread occurrence (in more than 20 localities) of polymictic subrounded to subangular faceted clasts with striations, sometimes in multiple sets; the generally massive, unbedded, poorly sorted and fine-grained matrix-supported nature of the diamictite; and the presence of associated varved shales with dropstones (Vanden Brande, 1936; Cahen, 1963, 1978; François, 1973; Binda and van Eden, 1974).

Because of the absence of subglacial striated pavements, very little is known about palaeoflow directions of the Neoproterozoic glaciers which deposited the Grand Conglomerat. Studies of the isopachs and facies in the Grand Conglomerat indicate that thin continental glacial moraines were situated in the north of the Lufilian arc, while to the south deposition was in the form of thicker glaciomarine facies (François, 1973; Binda & van Eden, 1974; Museu, 1987). In the Chambishi Basin, in borehole MJZC/9, the 26 m thick Grand Conglomerat is conformable with black shales and turbidites (109 m thick) of the underlying Mwashya Subgroup. Diamictites of the Grand Conglomerat are interbedded with turbidites, and are interpreted to have formed by sediment gravity flow processes in a glaciomarine basin (e.g., Benn & Evans, 1998).

d. Nguba Group- West Lunga Formation

To the southeast of the Mwinilunga area, strongly deformed and poorly differentiated Katangan rocks of the West Lunga Formation, comprising shales, dolomites, siltstones, diamictites, banded iron formations and porphyritic volcanics, have been provisionally correlated with the Lower Kundelungu Supergroup (Liyungu et al., 2001), which corresponds to the upper part of the Nguba Group above the Grand Conglomerat (i.e., Muombe Subgroup of Wendorff, 2003a,b). One of the porphyritic lavas in this area has been dated at 735 ± 5 Ma with the U/Pb SHRIMP technique on single zircon, but its exact stratigraphic position with respect to the Grand Conglomerat is problematical (Armstrong, 2000; Liyungu et al., 2001).

e. Kundelungu Group- Petit Conglomerat Formation

The Petit Conglomerat Formation forms the base of the Kundelungu Group, and may overlie the Nguba Group with an erosional unconformity (Wendorff, 2003b). The Petit Conglomerat diamicitite is, like the Grand Conglomerat, also of glacial origin (based on the abundant and widespread presence of faceted and striated clasts of both intrabasinal and extrabasinal origin; Vanden Brande, 1936; Cahen, 1978), and is overlain by a cap carbonate (the “Calcaire rose”).

f. Fungurume Group

The Fungurume Group is a newly defined unit in the Katanga Supergroup, regarded as a syntectonic foreland basin fill (Wendorff, 2003a), which rests unconformably on the Nguba Group. It consists of continental red beds of the Mutoshi Formation, previously called “RAT”; the Dipeta Formation consisting of marginal marine mixed clastic and carbonate rocks; and the Kambove Formation, comprising olistostromes deposited by subaqueous sediment-gravity flows (Wendorff, 2003a).

g. Biano Group

The Biano Group (Wendorff, 2003a,b), also known as Ks3 (François, 1973), Groupe du Biano (François, 1995), Plateau Group (Wendorff, 2001), or Plateaux Subgroup of the Kundelungu Group, Ku3 (Cailteux, 2003), was examined in outcrops 8 km NE of Gombela, in the Kundelungu Plateau National Park, Katanga, D.R. Congo. Here the uppermost Katangan sedimentary rocks consist entirely of red siltstones which are rippled.

The uppermost Katangan sediments of the Biano Group in the Kundelungu Plateau consist entirely of red siltstones which are ripple marked, with very thin (< 1 cm) shaley interbeds. The shales show evidence of exposure and desiccation in the form of mudcracks, and have been reworked as mudchip conglomerates in rippled siltstones. Some of the ripples are flat-topped, and indicate modification during falling water levels.

The ripples show internal cross laminations (Figure 2), and they are current ripples. The polymodal palaeocurrents (based on 53 measurements on current ripples from 8 stations) were mainly southerly and southwesterly, with minor modes to the west-northwest and north (Figure 3). These siltstones are unmetamorphosed, and contain abundant detrital muscovites (Figure 4), which glisten on bedding plane surfaces. The red siltstones of the Biano Group may correlate with the uppermost redbeds within the Luapula Beds of northwestern Zambia (Abraham, 1959; Thieme, 1971).

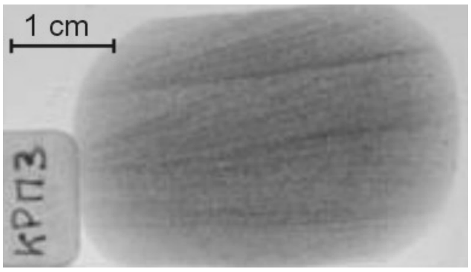

Figure 2. Photograph of a thin-section of a ripple-marked siltstone (sample KPM3), showing ripple cross-laminations, from the Biano Group, 8 km NE of Gombela, Kundelungu Plateau National Park, D. R. Congo.

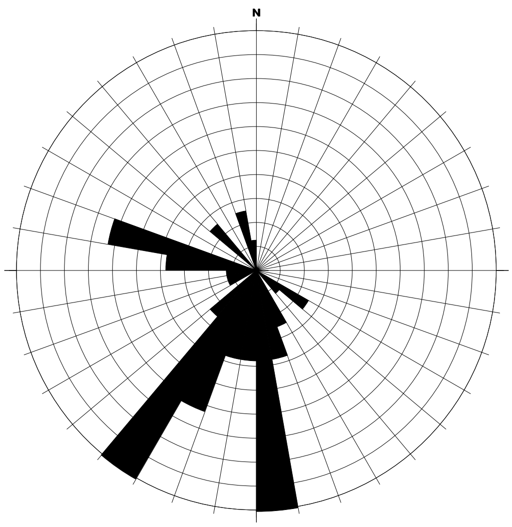

Figure 3. Rose diagram showing palaeocurrent trends measured from 53 sets of current ripples in siltstones from the Biano Group, 8 km NE of Gombela, Kundelungu Plateau National Park, D. R. Congo. Each concentric ring represents one percent of the measured population of the data set.

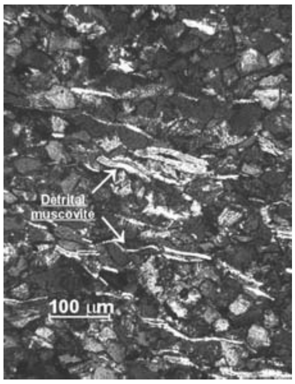

Figure 4. Photomicrograph of sample KPM3, showing abundant detrital muscovite laths (arrowed) which are curved due to compaction between smaller detrital quartz grains.

4. Analytical techniques

U-Pb analyses were performed on the SHRIMP I at the Australian National University, Canberra. The separation of zircons was carried out at the Hugh Allsopp Laboratory, Johannesburg, South Africa, using conventional techniques. The SHRIMP analytical procedure used in this study is similar to that described by Claoué-Long et al. (1995). Age calculations and plotting were done using Isoplot/Ex (Ludwig, 2000) and all ages are quoted with errors at 1σ. In the age interpretations, only isotopic ratios that are 10% or less discordant were considered as reliable age indicators. Highly discordant data were not discarded but evaluated case by case.

^{40}Ar-^{39}Ar analyses were performed at the Australian National University, Canberra. Muscovites were separated at the the Hugh Allsopp Laboratory, Johannesburg, South Africa and extracts were purified at the Australian National University. Crystals were placed into an aluminium irradiation canister together with interspersed aliquots of the flux monitor GA 1550 (age = 98.5 Ma; Spell & McDougall, 2003). Packets containing degassed potassium glass were placed at either end of the canister to monitor the ^{40}Ar production from potassium (e.g. Tetley, 1980). The irradiation canister was irradiated for 504 hours in position X34 of the ANSTO, HIFAR reactor, Lucas Heights, New South Wales, Australia. The canister, which was lined with 0.2 mm Cd to absorb thermal neutrons, was inverted three times during the irradiation, which reduced neutron flux gradients to < 2% along the length of the canister. Mass discrimination was monitored by analyses of standard air volumes. Correction factors for interfering reactions are as follows: $(^{40}Ar/^{39}Ar)_{Ca}$ = 3.50(± 0.14)x10^{-4}; $(^{39}Ar/^{37}Ar)_{Ca}$ = 7.86 (± 0.01) x 10^{-4} (McDougall & Harrison, 1999); $(^{40}Ar/^{39}Ar)_{K}$ = 0.050 (± 0.005). K/Ca ratios were determined from the ANU laboratory hornblende standard 77-600 and were calculated as follow: K/Ca = 1.9 x $^{39}Ar/^{37}Ar$. The reported data have been corrected for system blanks, mass discrimination and radioactive decay. The calculated ages have been additionally corrected for reactor interferences, fluence gradients and atmospheric contamination. Errors associated with the age determinations are one sigma uncertainties and include errors in the J-value estimates. The error on the J-value is ± 0.35 %, excluding the uncertainty in the age of GA1550 (which is ~ 1%). Decay constants are those of Steiger and Jäger (1977).

5. Results

a. Lower Roan Subgroup

Detrital zircons from four arkosic sandstone samples of the Lower Roan Subgroup from Musoshi (samples SPOTMU and MUS3), Konkola (sample KNS7), and the Chambishi Basin (sample RCB2/4) (Figure 1) were U-Pb dated with the SHRIMP. Most of the samples have zircons almost exclusively of Palaeoproterozoic age with a few younger ages. 54 zircons (55 analyses) from SPOTMU and 10 zircons from MUS3 were analysed. Results are shown in concordia plots Figures 5 and 6 and are listed in Tables 2 and 3. Out of 55 analyses on SPOTMU, 7 were more than 10% discordant, and were not taken into account during the discussion. The discordant analyses are, however, plotted on the concordia diagram. The other 48 analyses plot in a large cluster of $^{207}Pb/^{206}Pb$ ages ranging from 2081 ± 27 Ma to 1789 ± 35 Ma. The same cluster is found with the sample MUS3 (Figure 6) with $^{207}Pb/^{206}Pb$ ages ranging from 2066 ± 20 Ma to 1883 ± 21Ma. The sample from Konkola (KNS7, 14 analyses) yielded a similar detrital zircon age range to the Musoshi samples, from 1996 ± 15 Ma to 1836 ± 26 (Table 4, Figure 7). For the sample RCB2/4, due to technical problems related to the SHRIMP, out of 50 analyses, 18 were completed and could be plotted on a concordia diagram (Table 5, Figure 8). 14 out of 18 analyses plot on the concordia diagram in a cluster with Palaeoproterozoic ages ranging from 1813 ± 28 Ma to 2062 ± 38 Ma. Four analyses show different ages and different degrees of concordancy. Two ages are Neoproterozoic with 891 ± 199 Ma (115% concordant) and 908 ± 40 Ma (analyses 13.1 and 17.2). The two remaining analyses are Mesoproterozoic in age at 1301 ± 46 Ma (analysis 4.1) and 1152 ± 65 Ma (analysis 17.1).

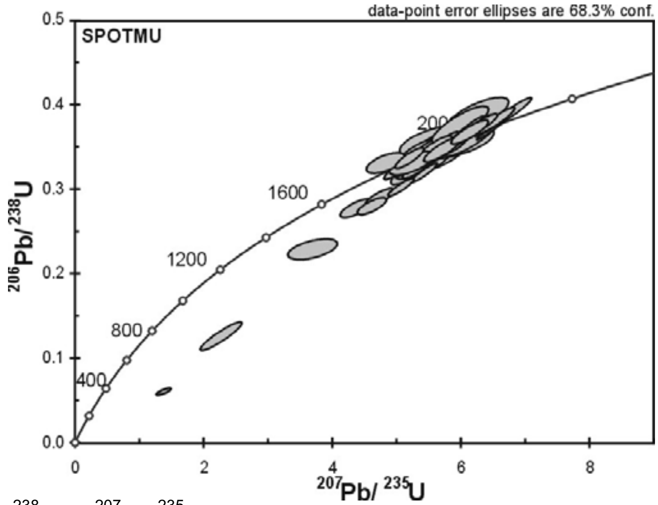

Figure 5. $^{206}Pb/^{238}U$ vs $^{207}Pb/^{235}U$ concordia plot of ages (Ma) of detrital zircons from lower Roan Group arkose at Musoshi Mine, D. R. Congo (sample SPOTMU).

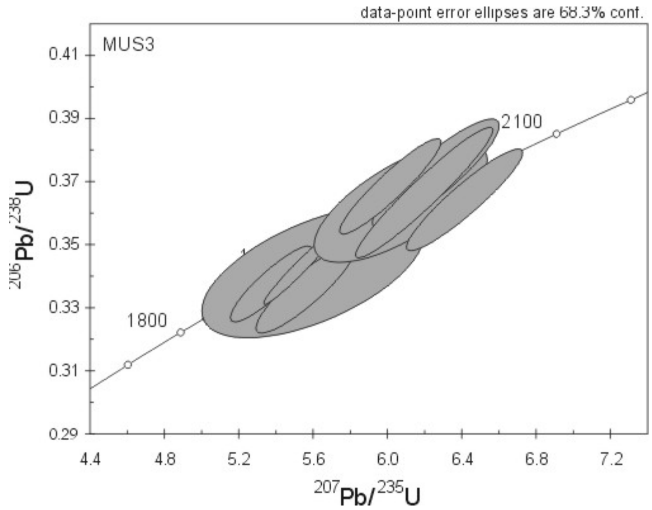

Figure 6. $^{206}Pb/^{238}U$ vs $^{207}Pb/^{235}U$ concordia plot of ages (Ma) of detrital zircons from lower Roan Group arkose at Musoshi Mine, D. R. Congo (sample MUS3).

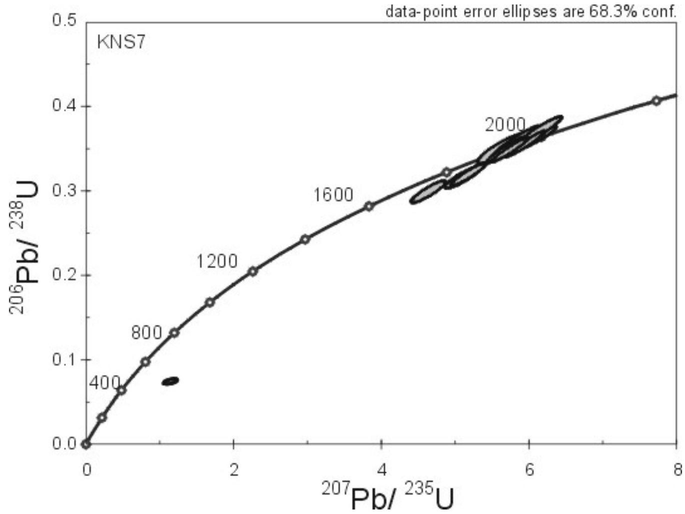

Figure 7. $^{206}Pb/^{238}U$ vs $^{207}Pb/^{235}U$ concordia plot of ages (Ma) of detrital zircons from lower Roan Group arkose at Konkola Mine, Zambia (sample KNS7).

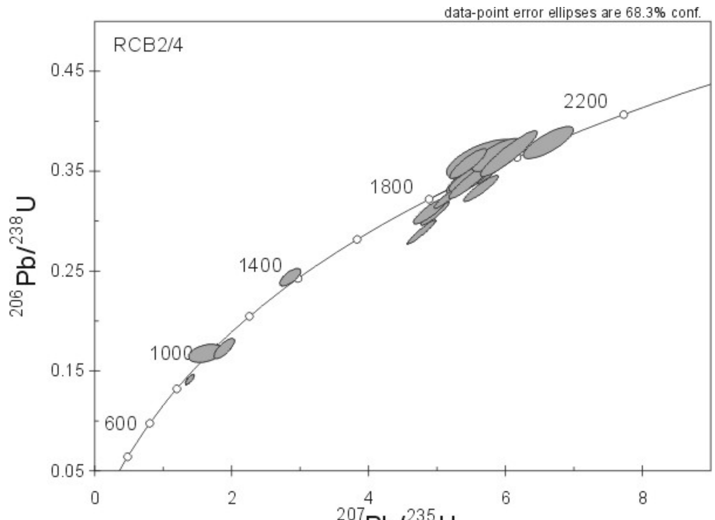

Figure 8. $^{206}Pb/^{238}U$ vs $^{207}Pb/^{235}U$ concordia plot of ages (Ma) of detrital zircons from lower Roan Group arkose from borehole RCB2, 1467.8 m depth, in the Chambishi Basin, Zambian Copperbelt (sample RCB2/4).

Table 2. Summary of SHRIMP U-Th-Pb zircon results for sample SPOTMU.

							Radiogenic Ratios						Ages (in Ma)						
Grain. spot	U (ppm)	Th (ppm)	Th/U	Pb* (ppm)	$^{204}Pb/^{206}Pb$	f_{206} %	$^{206}Pb/^{238}U$	±	$^{207}Pb/^{235}U$	±	$^{207}Pb/^{206}Pb$	±	$^{206}Pb/^{238}U$	±	$^{207}Pb/^{235}U$	±	$^{207}Pb/^{206}Pb$	±	Conc. %
1.2	84	67	0.79	34	0.00047	0.726	0.3480	0.0136	5.817	0.266	0.1213	0.0024	1887	95	1925	65	1949	40	98
2	85	79	0.93	36	0.00037	0.562	0.3521	0.0139	5.678	0.313	0.1170	0.0040	1977	114	1945	66	1928	49	102
3	492	82	0.17	167	0.00021	0.320	0.3390	0.0216	5.524	0.406	0.1182	0.0035	1908	283	1882	105	1904	65	98
3.2	213	145	0.68	83	0.00028	0.429	0.3444	0.0082	5.648	0.156	0.1189	0.0013	1870	57	1908	40	1923	24	98
4	116	138	1.19	48	0.00045	0.692	0.3352	0.0098	5.107	0.203	0.1105	0.0026	1724	64	1864	47	1837	34	103
5	94	66	0.70	37	0.00042	0.642	0.3515	0.0114	5.812	0.234	0.1199	0.0024	1852	84	1942	55	1948	35	99
6	57	44	0.77	25	0.00054	0.828	0.3870	0.0132	6.256	0.313	0.1173	0.0038	1993	122	2109	62	2012	45	110
7	87	96	1.11	36	0.00037	0.570	0.3386	0.0109	5.697	0.253	0.1220	0.0033	1748	79	1880	53	1931	39	95
8	65	81	1.24	20	0.00170	2.597	0.2315	0.0079	3.694	0.253	0.1157	0.0064	1535	78	1343	42	1570	56	71
9	62	129	2.07	30	0.00049	0.748	0.3303	0.0117	5.383	0.282	0.1182	0.0041	1837	83	1840	57	1882	46	95
10	584	411	0.70	200	0.00041	0.635	0.3200	0.0074	5.414	0.140	0.1227	0.0011	1114	34	1790	36	1887	22	90
11	303	157	0.52	53	0.00174	2.666	0.1313	0.0107	2.269	0.210	0.1253	0.0044	1999	181	795	61	1203	67	39
12	364	410	1.13	124	0.00062	0.947	0.2790	0.0073	4.368	0.165	0.1135	0.0028	1455	52	1587	37	1706	32	85
13	277	311	1.12	118	0.00022	0.341	0.3456	0.0086	5.411	0.150	0.1135	0.0011	1885	51	1914	41	1887	24	103
14	141	121	0.85	58	0.00075	1.149	0.3558	0.0101	5.417	0.220	0.1104	0.0029	1851	75	1962	48	1888	35	109
15	399	36	0.09	127	0.00035	0.536	0.3251	0.0078	5.323	0.153	0.1188	0.0015	1293	208	1814	38	1873	25	94
16	46	45	0.98	20	0.00167	2.556	0.3561	0.0139	5.778	0.483	0.1177	0.0081	2085	157	1964	67	1943	75	102
17	180	142	0.79	69	0.00040	0.609	0.3301	0.0076	5.136	0.214	0.1128	0.0036	1863	68	1839	37	1842	36	100
18	115	128	1.11	51	0.00073	1.116	0.3566	0.0098	5.767	0.268	0.1173	0.0040	1958	76	1966	47	1942	41	103
19	231	134	0.58	97	0.00023	0.353	0.3797	0.0101	5.990	0.184	0.1144	0.0014	2037	69	2075	48	1974	27	111
20	187	178	0.95	78	0.00001	0.015	0.3507	0.0090	5.509	0.161	0.1140	0.0013	1896	57	1938	43	1902	25	104
21	336	305	0.91	128	0.00038	0.590	0.3241	0.0081	5.021	0.147	0.1124	0.0014	1707	49	1810	39	1823	25	98
22	225	199	0.88	93	0.00024	0.370	0.3529	0.0085	5.545	0.155	0.1140	0.0013	1928	54	1949	40	1908	24	105
23	80	64	0.79	35	0.00044	0.675	0.3711	0.0110	6.231	0.238	0.1218	0.0025	2006	84	2035	52	2009	34	103
24	514	373	0.72	193	0.00007	0.114	0.3323	0.0072	5.197	0.164	0.1134	0.0023	1742	121	1850	35	1852	27	100
25	236	28	0.12	84	0.00014	0.209	0.3607	0.0088	5.952	0.163	0.1197	0.0012	1948	132	1986	42	1969	24	102
26	266	258	0.97	86	0.00106	1.618	0.2918	0.0069	4.733	0.148	0.1176	0.0021	981	37	1651	34	1773	27	86
27	97	79	0.81	41	0.00022	0.341	0.3583	0.0127	6.127	0.265	0.1240	0.0026	1987	85	1974	61	1994	38	98
28	109	47	0.43	42	0.00043	0.665	0.3622	0.0105	5.913	0.239	0.1184	0.0030	1858	120	1992	50	1963	36	103

Notes :

1. Uncertainties given at the one s level.
2. f_{206} % denotes the percentage of ^{206}Pb that is common Pb.
3. Correction for common Pb made using the measured $^{204}Pb/^{206}Pb$ ratio.
4. For % Conc., 100% denotes a concordant analysis.

Table 2. Summary of SHRIMP U-Th-Pb zircon results for sample SPOTMU (cont.).

							Radiogenic Ratios						Ages (in Ma)						
Grain. spot	U (ppm)	Th (ppm)	Th/U	Pb* (ppm)	$^{204}Pb/^{206}Pb$	f_{206} %	$^{206}Pb/^{238}U$	±	$^{207}Pb/^{235}U$	±	$^{207}Pb/^{206}Pb$	±	$^{206}Pb/^{238}U$	±	$^{207}Pb/^{235}U$	±	$^{207}Pb/^{206}Pb$	±	Conc. %
29	2203	2202	1.00	196	0.00995	15.24	0.0674	0.0026	1.380	0.071	0.1485	0.0045	516	27	420	16	880	31	18
30	115	178	1.55	52	0.00032	0.489	0.3397	0.0115	5.524	0.228	0.1180	0.0024	1838	76	1885	55	1904	36	98
31	507	285	0.56	156	0.00091	1.387	0.3033	0.0069	5.065	0.132	0.1211	0.0013	640	33	1708	34	1830	22	87
32	351	66	0.19	132	0.00005	0.074	0.3731	0.0098	6.512	0.179	0.1266	0.0007	1881	65	2044	46	2048	25	100
33	123	133	1.08	56	0.00010	0.157	0.3676	0.0103	6.186	0.192	0.1220	0.0013	2044	64	2018	49	2003	28	102
34	206	204	0.99	81	0.00015	0.227	0.3290	0.0090	5.206	0.162	0.1148	0.0013	1804	57	1834	44	1854	27	98
35	92	137	1.49	42	0.00041	0.634	0.3423	0.0106	5.312	0.218	0.1126	0.0026	1874	71	1898	51	1871	36	103
36	178	123	0.69	70	0.00014	0.217	0.3452	0.0084	5.748	0.158	0.1208	0.0012	1876	55	1911	40	1939	24	97
37	100	158	1.58	47	0.00066	1.017	0.3501	0.0099	5.688	0.259	0.1178	0.0038	1884	72	1935	47	1930	40	101
38	225	255	1.13	93	0.00026	0.402	0.3342	0.0078	5.135	0.144	0.1114	0.0014	1816	47	1859	38	1842	24	102
39	93	109	1.17	43	0.00063	0.966	0.3750	0.0143	5.985	0.292	0.1158	0.0030	1937	91	2053	68	1974	43	109
40	269	205	0.76	108	0.00034	0.515	0.3537	0.0087	5.716	0.160	0.1172	0.0013	1867	55	1952	41	1934	24	102
41	230	217	0.95	92	0.00004	0.061	0.3354	0.0088	5.385	0.153	0.1164	0.0009	1885	57	1864	43	1882	25	98
42	209	217	1.04	89	0.00015	0.233	0.3483	0.0093	5.577	0.182	0.1161	0.0018	1958	63	1927	45	1913	29	102
43	605	952	1.57	189	0.00135	2.063	0.2815	0.0065	4.609	0.149	0.1187	0.0024	617	24	1599	33	1751	27	83
44	150	184	1.23	56	0.00080	1.225	0.3308	0.0091	5.225	0.227	0.1146	0.0035	1001	55	1842	44	1857	38	98
45	320	219	0.69	136	0.00021	0.316	0.3750	0.0085	6.449	0.168	0.1248	0.0013	2027	55	2053	40	2039	23	101
46	164	162	0.99	73	0.00008	0.128	0.3641	0.0113	6.092	0.205	0.1214	0.0012	2043	73	2002	54	1989	30	101
47	205	144	0.70	91	0.00024	0.375	0.3893	0.0112	6.765	0.212	0.1260	0.0012	2074	68	2120	52	2081	28	104
48	253	107	0.42	103	0.00030	0.459	0.3802	0.0100	6.535	0.193	0.1247	0.0013	1977	70	2077	47	2051	26	103
49	89	84	0.95	34	0.00111	1.696	0.3313	0.0078	4.824	0.197	0.1056	0.0032	1701	66	1845	38	1789	35	107
50	135	94	0.70	52	0.00050	0.770	0.3472	0.0096	5.710	0.194	0.1193	0.0020	1766	67	1921	46	1933	30	99
51	178	214	1.20	72	0.00041	0.633	0.3370	0.0081	5.194	0.151	0.1118	0.0015	1548	44	1872	39	1852	25	102
52	385	61	0.16	142	0.00012	0.186	0.3709	0.0093	6.092	0.161	0.1191	0.0008	1847	72	2033	44	1989	23	105
53	146	153	1.05	67	0.00030	0.455	0.3740	0.0093	6.288	0.182	0.1219	0.0015	2011	57	2048	44	2017	26	103
54	149	96	0.64	61	0.00024	0.368	0.3668	0.0092	6.129	0.188	0.1212	0.0018	1998	71	2015	44	1994	27	102

Notes :
1. Uncertainties given at the one s level.
2. f_{206} % denotes the percentage of ^{206}Pb that is common Pb.
3. Correction for common Pb made using the measured $^{204}Pb/^{206}Pb$ ratio.
4. For % Conc., 100% denotes a concordant analysis.

Table 3. Summary of SHRIMP U-Pb zircon results for sample MUS3.

							Radiogenic Ratios						Ages (in Ma)						
Grain. spot	**U (ppm)**	**Th (ppm)**	**Th/U**	**Pb* (ppm)**	**$^{204}Pb/^{206}Pb$**	**f_{206} %**	**$^{206}Pb/^{238}U$**	**±**	**$^{207}Pb/^{235}U$**	**±**	**$^{207}Pb/^{206}Pb$**	**±**	**$^{206}Pb/^{238}U$**	**±**	**$^{207}Pb/^{235}U$**	**±**	**$^{207}Pb/^{206}Pb$**	**±**	Conc. **%**
1.1	584	438	0.749	228	0.000289	0.46	0.3385	0.0078	5.377	0.145	0.1152	0.0013	1879	37	1881	23	1883	21	100
2.1	461	1036	2.247	243	0.000356	0.57	0.3366	0.0088	5.558	0.173	0.1198	0.0017	1871	43	1910	27	1953	25	96
3.1	1338	56	0.042	444	0.000135	0.21	0.3435	0.0075	5.533	0.128	0.1168	0.0006	1904	36	1906	20	1908	9	100
4.1	564	249	0.441	220	0.000229	0.35	0.3671	0.0091	6.053	0.165	0.1196	0.0010	2016	43	1984	24	1950	15	103
5.1	55	58	1.049	24	0.001023	1.57	0.3638	0.0123	6.075	0.307	0.1211	0.0041	2000	58	1987	45	1973	61	101
6.1	191	122	0.639	80	0.000074	0.11	0.3727	0.0112	6.264	0.225	0.1219	0.0020	2042	53	2013	32	1984	29	103
7.1	61	76	1.253	27	0.000431	0.69	0.3421	0.0134	5.605	0.395	0.1188	0.0064	1897	65	1917	63	1939	100	98
8.1	95	109	1.15	44	0.000010	0.02	0.3646	0.0104	6.418	0.206	0.1277	0.0015	2004	49	2035	29	2066	20	97
9.1	124	107	0.859	54	0.000010	0.02	0.3669	0.0133	6.202	0.243	0.1226	0.0014	2015	63	2005	35	1995	20	101
10.1	310	187	0.604	127	0.000156	0.24	0.3688	0.0098	6.019	0.180	0.1184	0.0012	2024	47	1979	26	1932	19	105

Notes :

1. Uncertainties given at the one s level.
2. f_{206} % denotes the percentage of ^{206}Pb that is common Pb.
3. Correction for common Pb made using the measured $^{204}Pb/^{206}Pb$ ratio.
4. For % Conc., 100% denotes a concordant analysis.

Table 4. Summary of SHRIMP U-Th-Pb zircon results for sample KNS7.

Grain. spot	U (ppm)	Th (ppm)	Th/U	Pb* (ppm)	^{204}Pb/^{206}Pb	f_{206} %	Radiogenic Ratios ^{206}Pb/^{238}U	±	^{207}Pb/^{235}U	±	^{207}Pb/^{206}Pb	±	Ages (in Ma) ^{206}Pb/^{238}U	±	^{207}Pb/^{235}U	±	^{207}Pb/^{206}Pb	±	Conc. %
1.1	612	456	0.74	253	0.000008	0.01	0.3594	0.0066	5.964	0.114	0.1204	0.0004	1979	31	1971	17	1962	6	101
2.1	472	498	1.05	210	0.000038	0.06	0.3630	0.0065	5.970	0.110	0.1193	0.0004	1997	31	1971	16	1945	6	103
3.1	125	186	1.49	60	0.000010	0.02	0.3636	0.0081	6.152	0.152	0.1227	0.0010	1999	39	1998	22	1996	15	100
4.1	615	365	0.59	251	0.000017	0.03	0.3684	0.0065	6.130	0.115	0.1207	0.0005	2022	31	1995	16	1966	7	103
5.1	881	1458	1.65	83	0.005180	8.29	0.0805	0.0021	1.153	0.060	0.1039	0.0043	499	12	779	29	1694	79	30
6.1	663	230	0.35	232	0.000013	0.02	0.3361	0.0090	5.450	0.155	0.1176	0.0008	1868	43	1893	25	1920	13	97
7.1	307	102	0.33	100	0.000384	0.61	0.3169	0.0084	5.115	0.161	0.1171	0.0016	1775	41	1839	27	1912	25	93
8.1	227	132	0.58	87	0.000315	0.50	0.3506	0.0117	5.664	0.226	0.1171	0.0021	1938	56	1926	35	1913	33	101
9.1	248	176	0.71	99	0.000117	0.19	0.3588	0.0117	5.847	0.209	0.1182	0.0013	1976	56	1953	31	1929	20	103
10.1	320	137	0.43	126	0.000061	0.10	0.3708	0.0111	6.160	0.203	0.1205	0.0012	2033	53	1999	29	1963	19	104
11.1	414	283	0.68	147	0.000186	0.30	0.3204	0.0085	5.195	0.154	0.1176	0.0012	1792	42	1852	26	1920	19	93
12.1	295	421	1.42	114	0.000254	0.41	0.3002	0.0084	4.646	0.153	0.1123	0.0016	1692	42	1758	28	1836	26	92
13.1	333	307	0.92	136	0.000144	0.23	0.3486	0.0092	5.691	0.163	0.1184	0.0009	1928	44	1930	25	1932	14	100
14.1	212	126	0.59	84	0.000010	0.02	0.3555	0.0098	5.966	0.176	0.1217	0.0009	1961	47	1971	26	1982	13	99
15.1	311	158	0.51	118	0.000118	0.19	0.3488	0.0093	5.761	0.164	0.1198	0.0009	1929	44	1941	25	1953	14	99

Notes :

1. Uncertainties given at the one σ level.
2. f_{206} % denotes the percentage of ^{206}Pb that is common Pb.
3. Correction for common Pb made using the measured ^{204}Pb/^{206}Pb ratio.
4. For % Conc., 100% denotes a concordant analysis.

Table 5. Summary of SHRIMP U-Pb zircon results for sample RCB2/4

							Radiogenic Ratios						Ages (in Ma)						
Grain. spot	U (ppm)	Th (ppm)	Th/U	Pb* (ppm)	$^{204}Pb/^{206}Pb$	f_{206} %	$^{206}Pb/^{238}U$	±	$^{207}Pb/^{235}U$	±	$^{207}Pb/^{206}Pb$	±	$^{206}Pb/^{238}U$	±	$^{207}Pb/^{235}U$	±	$^{207}Pb/^{206}Pb$	±	Conc. %
1.1	637.7	389	0.61	218	0.000038	0.06	0.3089	0.0076	4.981	0.137	0.1169	0.0011	1735	38	1816	24	1910	17	91
2.1	720.4	273.4	0.38	266	0.000067	0.11	0.3499	0.0074	5.806	0.133	0.1204	0.0008	1934	36	1947	20	1962	11	99
3.1	180.7	183.2	1.01	70	0.000050	0.08	0.3111	0.0082	4.909	0.156	0.1144	0.0017	1746	41	1804	27	1871	26	93
4.1	492.1	298.5	0.61	131	0.000158	0.25	0.2462	0.0057	2.865	0.100	0.0844	0.0020	1419	29	1373	27	1301	46	109
5.1	166.2	189.6	1.14	71	0.000185	0.30	0.3418	0.0094	5.466	0.206	0.1160	0.0026	1895	45	1895	33	1895	41	100
6.1	570.6	528	0.93	220	0.000159	0.26	0.3250	0.0071	5.170	0.127	0.1154	0.0010	1814	35	1848	21	1886	16	96
7.1	119.5	129	1.08	25	0.000813	1.30	0.1717	0.0059	1.628	0.164	0.0688	0.0062	1022	32	981	65	891	199	115
8.1	564.5	530.4	0.94	199	0.000033	0.05	0.2907	0.0079	4.787	0.141	0.1194	0.0010	1645	40	1783	25	1948	15	85
9.1	335.5	393.9	1.17	145	0.000216	0.35	0.3429	0.0079	5.429	0.156	0.1148	0.0017	1901	38	1890	25	1877	26	101
10.1	233.4	79.95	0.34	93	0.000333	0.53	0.3785	0.0103	6.646	0.244	0.1274	0.0027	2069	48	2066	33	2062	38	100
11.1	162.3	113.3	0.7	63	0.000062	0.10	0.3420	0.0124	5.528	0.223	0.1172	0.0016	1896	60	1905	35	1914	25	99
12.1	407.9	123.3	0.3	141	0.000228	0.37	0.3335	0.0085	5.655	0.166	0.1230	0.0014	1855	41	1925	26	2000	21	93
13.1	1191	672.8	0.56	187	0.000062	0.10	0.1462	0.0032	1.398	0.043	0.0693	0.0013	880	18	888	18	908	40	97
14.1	127.3	232.7	1.83	65	0.000591	0.95	0.3663	0.0106	5.884	0.238	0.1165	0.0029	2012	50	1959	36	1903	45	106
15.1	307	221.1	0.72	124	0.000379	0.61	0.3579	0.0096	5.469	0.177	0.1109	0.0017	1972	46	1896	28	1813	28	109
16.1	132.5	150	1.13	61	0.000040	0.06	0.3677	0.0148	6.072	0.276	0.1198	0.0020	2019	70	1986	40	1953	30	103
17.2	83.21	148.2	1.78	21	0.000010	0.02	0.1766	0.0066	1.905	0.099	0.0782	0.0025	1049	36	1083	35	1152	65	91
18.2	120.6	178.2	1.48	58	0.000740	1.18	0.3618	0.0131	5.698	0.356	0.1142	0.0053	1991	62	1931	55	1867	87	107
19.1	119.3	137.8	1.16	37	0.000288	0.46	0.3535	0.0127	*	*	*	*	1951	61			*		
20.1	185.4	235.1	1.27	64	0.000396	0.63	0.3807	0.0125	*	*	*	*	2080	59			*		
21.1	119.8	73.51	0.61	39	0.000538	0.86	0.3576	0.0105	*	*	*	*	1971	50			*		
22.1	246.3	133.1	0.54	82	0.000315	0.50	0.3721	0.0102	*	*	*	*	2039	48			*		
23.1	222.8	117.2	0.53	80	0.000367	0.59	0.4020	0.0131	*	*	*	*	2178	61			*		
24.1	240.8	260.7	1.08	81	0.000364	0.58	0.3728	0.0093	*	*	*	*	2042	44			*		
25.1	318	203.6	0.64	109	0.000219	0.35	0.3809	0.0098	*	*	*	*	2081	46			*		

Notes :

1. Uncertainties given at the one s level.
2. f_{206} % denotes the percentage of ^{206}Pb that is common Pb.
3. Correction for common Pb made using the measured $^{204}Pb/^{206}Pb$ ratio.
4. For % Conc., 100% denotes a concordant analysis.
5. * No 207Pb/206Pb or 207Pb/235U data available as 207Pb peak was not measured

Table 5. Summary of SHRIMP U-Pb zircon results for sample RCB2/4

							Radiogenic Ratios						Ages (in Ma)						
Grain. spot	U (ppm)	Th (ppm)	Th/U	Pb* (ppm)	$^{204}Pb/^{206}Pb$	f_{206} %	$^{206}Pb/^{238}U$	±	$^{207}Pb/^{235}U$	±	$^{207}Pb/^{206}Pb$	±	$^{206}Pb/^{238}U$	±	$^{207}Pb/^{235}U$	±	$^{207}Pb/^{206}Pb$	±	Conc. %
26.1	134.9	101.6	0.75	42	0.000482	0.77	0.3477	0.0099	*	*	*	*	1924	47			*		
27.1	1466	293.5	0.2	416	0.000136	0.22	0.3147	0.0067	*	*	*	*	1764	33			*		
28.1	191.6	110.1	0.57	70	0.001071	1.71	0.3983	0.0116	*	*	*	*	2161	54			*		
29.1	110.3	66.8	0.61	34	0.000744	1.19	0.3526	0.0116	*	*	*	*	1947	55			*		
30.1	568.4	246.7	0.43	154	0.000176	0.28	0.3040	0.0072	*	*	*	*	1711	36			*		
31.1	204.3	155.2	0.76	86	0.000155	0.25	0.4581	0.0159	*	*	*	*	2431	71			*		
32.1	403.9	107.9	0.27	111	0.000302	0.48	0.3092	0.0093	*	*	*	*	1737	46			*		
33.1	125.7	63.35	0.5	40	0.000727	1.16	0.3538	0.0107	*	*	*	*	1953	51			*		
34.1	327.7	95.19	0.29	122	0.000039	0.06	0.4067	0.0105	*	*	*	*	2200	48			*		
35.1	279.6	247.4	0.88	94	0.000245	0.39	0.3536	0.0110	*	*	*	*	1952	53			*		
36.1	475.9	327.1	0.69	148	0.000254	0.41	0.3286	0.0081	*	*	*	*	1831	40			*		
37.1	312.7	233.5	0.75	110	0.000231	0.37	0.3755	0.0100	*	*	*	*	2055	47			*		
38.1	44.82	76.2	1.7	13	0.003623	5.80	0.3078	0.0200	*	*	*	*	1730	100			*		
39.1	248.9	103.5	0.42	128	0.000196	0.31	0.5536	0.0166	*	*	*	*	2840	69			*		
40.1	168.6	164	0.97	55	0.000526	0.84	0.3689	0.0112	*	*	*	*	2024	53			*		
41.1	300	85.39	0.28	100	0.000285	0.46	0.3702	0.0089	*	*	*	*	2030	42			*		
42.1	746.9	328.1	0.44	250	0.000132	0.21	0.3666	0.0078	*	*	*	*	2013	37			*		
43.1	675.2	392.5	0.58	198	0.000245	0.39	0.3253	0.0073	*	*	*	*	1815	36			*		
44.1	345.8	156.4	0.45	111	0.000241	0.39	0.3548	0.0090	*	*	*	*	1957	43			*		
45.1	285.2	40.78	0.14	100	0.000374	0.60	0.3944	0.0121	*	*	*	*	2143	56			*		
46.1	507.8	188.3	0.37	184	0.000226	0.36	0.3974	0.0088	*	*	*	*	2157	41			*		
47.1	232.2	8.34	0.04	44	0.000807	1.29	0.2199	0.0058	*	*	*	*	1282	31			*		
48.1	577.4	460.9	0.8	201	0.000063	0.10	0.3741	0.0096	*	*	*	*	2049	45			*		
49.1	202	125.7	0.62	107	0.000359	0.57	0.5576	0.0145	*	*	*	*	2857	60			*		
50.1	184.6	93.24	0.51	61	0.000898	1.44	0.3566	0.0095	*	*	*	*	1966	45			*		

Notes :

1. Uncertainties given at the one s level.
2. f_{206} % denotes the percentage of ^{206}Pb that is common Pb.
3. Correction for common Pb made using the measured $^{204}Pb/^{206}Pb$ ratio.
4. For % Conc., 100% denotes a concordant analysis.
5. * No 207Pb/206Pb or 207Pb/235U data available as 207Pb peak was not measured

b. Nguba Group- Mwashya Subgroup

In the Mwashya Subgroup, the pyroclastics, mainly mafic lapilli tuffs and agglomerates of tholeiitic subalkaline basaltic composition, are best developed at Shituru Mine near Likasi, D. R. Congo (Lefebvre, 1974). An attempt was made to date zircons from these pyroclastics (sample S11), but they turned out to be entirely xenocrystic, with ages ranging from 3225 to 1068 Ma (Rainaud et al., 2003). Another sample (S27-S32) of Mwashya tuff from borehole S1 (depth 104.70m to 106.50m) at Shituru Mine yielded three xenocrystic zircon grains with U-Pb SHRIMP ages of 1870 ± 15, 1047 ± 25 and 983 ± 50 Ma (Table 6), reflecting inheritance from Palaeoproterozoic and Kibaran rocks.

c. Nguba Group- Grand Conglomerat

At Kipushi Mine, the Grand Conglomerat in the Nguba Group is intersected in borehole KHI 1150/34/HZ-S (Tshileo et al., 2003). In this horizontal borehole, 138 m of steeply dipping Kakontwe carbonates overlie the >118 m thick Grand Conglomerat, which consists of massive diamictite with mainly small lithic clasts, between 1 and 10 mm, together with larger granitoid clasts up to 15 cm across, supported in an argillitic matrix. We dated a suite of detrital zircons from a composite sample of the Grand Conglomerat from the borehole at Kipushi Mine (sample K30-41, 151-207 m). These detrital zircons have ages ranging from Palaeoproterozoic to Neoproterozoic (Table 7, Figure 9), as follows: 1945 ± 15 – 1846 ± 22 Ma (6 zircons); and 1025 ± 86 – 822 ± 42 Ma (4 zircons). One zircon gave an age of 729 ± 50 Ma, but it was only 88% concordant.

Table 6. Summary of SHRIMP U-Th-Pb zircon results for sample S27-S32.

Grain. spot	U (ppm)	Th (ppm)	Th/U	Pb* (ppm)	$^{204}Pb/^{206}Pb$	f_{206} %	Radiogenic Ratios $^{206}Pb/^{238}U$	±	$^{207}Pb/^{235}U$	±	$^{207}Pb/^{206}Pb$	±	Ages (in Ma) $^{206}Pb/^{238}U$	±	$^{207}Pb/^{235}U$	±	$^{207}Pb/^{206}Pb$	±	Conc. %
1.1	218	164	0.75	42	0.00006	0.11	0.1715	0.0034	1.755	0.043	0.0742	0.0009	1020	19	1029	16	1047	25	97
2.1	276	306	1.11	55	0.00048	0.83	0.1666	0.0033	1.651	0.055	0.0719	0.0017	993	18	990	21	983	50	101
3.1	248	89	0.36	86	0.00008	0.13	0.3322	0.0060	5.238	0.108	0.1144	0.0009	1849	29	1859	18	1870	15	99

Notes :
1. Uncertainties given at the one s level.
2. f_{206} % denotes the percentage of ^{206}Pb that is common Pb.
3. Correction for common Pb made using the measured $^{204}Pb/^{206}Pb$ ratio.
4. For % Conc., 100% denotes a concordant analysis.

Table 7. Summary of SHRIMP U-Pb zircon results for sample K30-41

							Radiogenic Ratios						Ages (in Ma)						
Grain. spot	U (ppm)	Th (ppm)	Th/U	Pb* (ppm)	$^{204}Pb/^{206}Pb$	f_{206} %	$^{206}Pb/^{238}U$	±	$^{207}Pb/^{235}U$	±	$^{207}Pb/^{206}Pb$	±	$^{206}Pb/^{238}U$	±	$^{207}Pb/^{235}U$	±	$^{207}Pb/^{206}Pb$	±	Conc. %
1.1	116	224	1.93	61	0.000135	0.21	0.3639	0.0107	5.910	0.213	0.1178	0.0021	2001	51	1963	32	1923	32	104
2.1	187	179	0.96	27	0.000141	0.25	0.1241	0.0035	1.141	0.045	0.0667	0.0016	754	20	773	21	827	50	91
3.1	214	140	0.65	30	0.000090	0.16	0.1274	0.0031	1.168	0.039	0.0665	0.0013	773	18	786	18	822	42	94
4.1	187	187	1.00	77	0.000026	0.04	0.3395	0.0084	5.282	0.152	0.1128	0.0014	1884	40	1866	25	1846	22	102
5.1	953	762	0.80	142	0.001586	2.72	0.1448	0.0032	1.419	0.061	0.0711	0.0024	872	18	897	26	960	71	91
6.1	87	46	0.53	17	0.000468	0.80	0.1878	0.0081	1.900	0.120	0.0734	0.0030	1109	44	1081	43	1025	86	108
7.1	273	151	0.55	107	0.000150	0.23	0.3566	0.0095	5.861	0.169	0.1192	0.0010	1966	45	1956	25	1945	15	101
8.1	94	136	1.46	19	0.000341	0.57	0.1534	0.0056	1.745	0.103	0.0825	0.0034	920	31	1025	39	1258	84	73
9.1	294	296	1.00	115	0.000036	0.06	0.3220	0.0083	5.067	0.146	0.1141	0.0012	1799	41	1831	25	1866	18	96
10.1	1772	278	0.16	188	0.000381	0.65	0.1109	0.0025	1.107	0.033	0.0724	0.0013	678	14	757	16	997	37	68
11.1*	58	90	1.55	10	0.001748	0.37	0.1248	0.0042	-	-	-	-	758	24	-	-	-	-	-
12.1	145	149	1.03	63	0.000282	0.43	0.3572	0.0092	5.818	0.178	0.1181	0.0016	1969	44	1949	27	1928	25	102
13.1	200	155	0.77	80	0.000101	0.16	0.3455	0.0118	5.590	0.219	0.1173	0.0018	1913	57	1915	34	1916	28	100
14.1	569	416	0.73	66	0.000308	0.54	0.1042	0.0027	0.914	0.034	0.0636	0.0015	639	16	659	18	729	50	88

Notes :

1. Uncertainties given at the one σ level.
2. f_{206} % denotes the percentage of ^{206}Pb that is common Pb.
3. Correction for common Pb made using the measured $^{204}Pb/^{206}Pb$ ratio, except for * where correction for common Pb made using the measured $^{238}U/^{206}Pb$ and 207Pb/206Pb ratios following Tera and Wasserburg (1972) as outlined in Compston et al. (1992).
4. For % Conc., 100% denotes a concordant analysis.

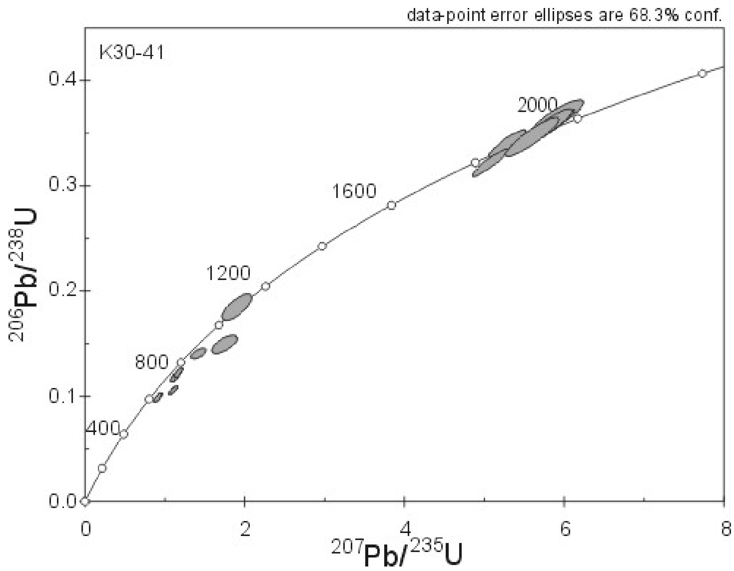

Figure 9. $^{206}Pb/^{238}U$ vs $^{207}Pb/^{235}U$ concordia plot of ages (Ma) of detrital zircons from a composite sample of the Grand Conglomerat, Nguba Group, at Kipushi Mine, D.R. Congo, intersected in borehole KHI 1150/34/HZ-S, at depths of between 151 and 207 m (sample K30-41).

d. Biano group

Detrital muscovites from these red siltstones of the Biano Group near Gombela were dated, using the laser $^{40}Ar/^{39}Ar$ technique. The detrital muscovite grains were too tiny to allow for step heating, therefore they were analysed using single-step laser fusion. The results of laser probe spot fusion of seven individual detrital muscovite grains show a range of $^{40}Ar/^{39}Ar$ ages between 638.3 ± 3.9 Ma and 572.6 ± 4.9 Ma, with one age of 1478.8 ± 5.1 Ma (Table 8, Figure 10). 50 detrital zircons from the same sample (KPM3) were dated using U-Pb (SHRIMP)- of these, 47 ages were <±10% discordant (Table 9, Figure 11). These ages range from 1977 ± 11 – 1780 ± 37 Ma (45 zircons) and 1219 ± 113 – 1176 ± 62 Ma (2 zircons).

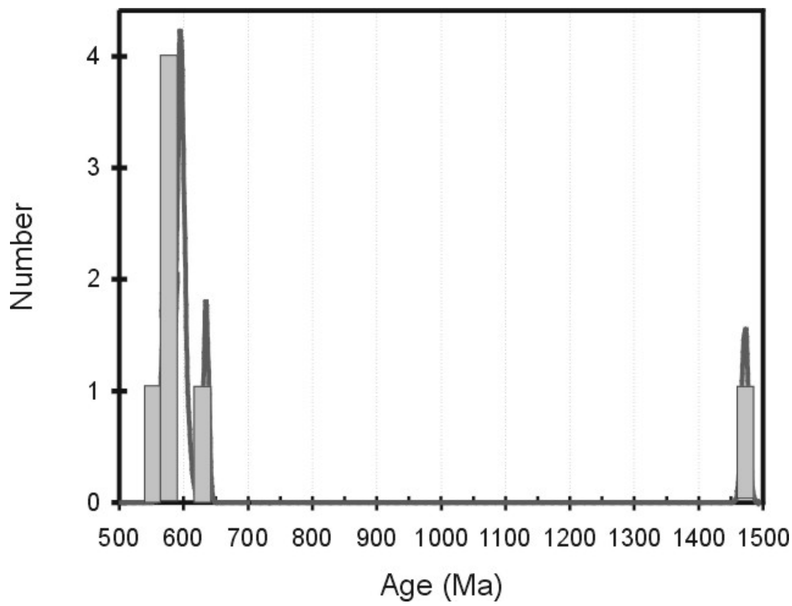

Figure 10. Histogram showing $^{40}Ar/^{39}Ar$ ages of individual detrital muscovite grains from a red siltstone of the Biano Group (sample KPM3), 8 km NE of Gombela, Kundelungu Plateau National Park, D. R. Congo

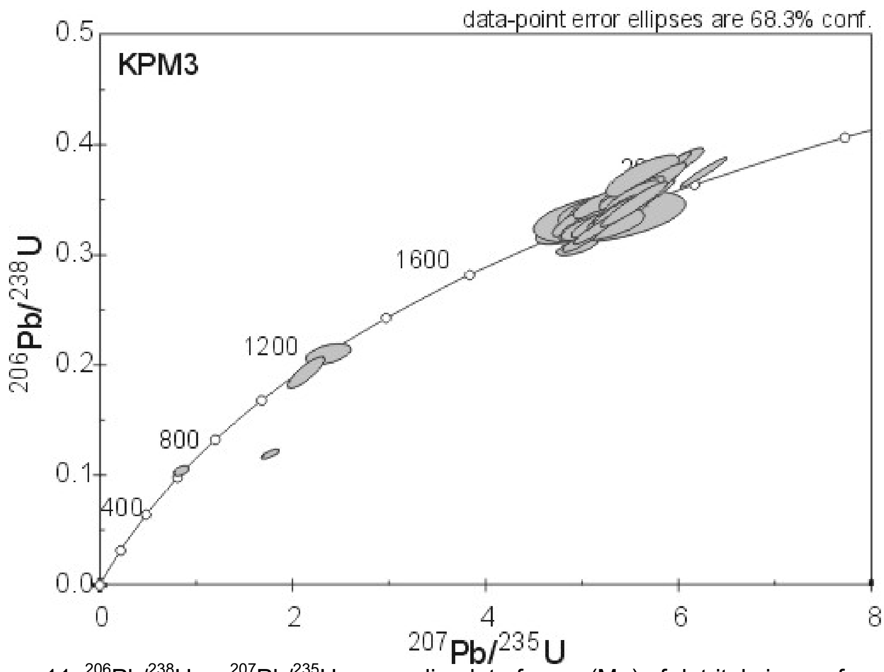

Figure 11. $^{206}Pb/^{238}U$ vs $^{207}Pb/^{235}U$ concordia plot of ages (Ma) of detrital zircons from a red siltstone of the Biano Group (sample KPM3), 8 km NE of Gombela, Kundelungu Plateau National Park, D. R. Congo.

Table 8. $^{40}Ar/^{39}Ar$ Laser Probe Analytical Results for Single Detrital Muscovite Grains from Sample KPM3.

Grain No.	Step No.	Cum. ^{39}Ar	$^{40}Ar/^{39}Ar$	±	$^{37}Ar/^{39}Ar$	±	$^{36}Ar/^{39}Ar$	±	Ca/K	±	Vol ^{39}Ar $x10^{-16}$mol	Rad. ^{40}Ar (%)	$^{40}Ar^*/^{39}Ar$	±	Age (Ma)	±
1	Fusion	1.00	38.76	0.19	0.032	0.027	0.0015	0.0006	0.061	0.051	1.890	98.69	38.26	0.27	596.9	3.9
2	Fusion	1.00	124.40	0.48	0.081	0.076	0.0016	0.0006	0.276	0.224	2.235	99.58	123.89	0.51	1478.8	5.1
3	Fusion	1.00	37.55	0.36	0.081	0.098	0.0011	0.0005	0.153	0.185	1.406	99.00	37.18	0.39	582.5	5.4
4	Fusion	1.00	39.42	0.35	0.020	0.009	0.0028	0.0003	0.039	0.018	1.775	97.76	38.54	0.36	600.6	5.0
5	Fusion	1.00	39.19	0.38	0.060	0.073	0.0019	0.0019	0.114	0.139	0.600	98.45	38.59	0.68	601.2	9.1
6	Fusion	1.00	36.94	0.27	0.103	0.084	0.0015	0.0008	0.197	0.160	1.400	98.67	36.45	0.35	572.6	4.9
7	Fusion	1.00	41.82	0.23	0.018	0.057	0.0012	0.0005	0.034	0.109	2.925	99.02	41.42	0.27	638.3	3.9

1. All data are corrected for mass spectrometer backgrounds, line blanks, mass discrimination and radioactive decay.
2. Weighted average of J from standards = 0.010249 ± 0.000031
2. Errors are reported as 1σ uncertainties; Errors associated with the ages include the 1σ uncertainty in the J-value.
3. Correction factors: $(^{36}Ar/^{37}Ar)_{Ca}$ = 3.5E-4; $(^{39}Ar/^{37}Ar)_{Ca}$ = 7.86E-4; $(^{40}Ar/^{39}Ar)_K$ = 0.058; Ca/K conversion factor = 1.9; λ ^{40}K = 5.543E-10

Table 9. Summary of SHRIMP U-Pb zircon results for sample KPM3

Grain. spot	U (ppm)	Th (ppm)	Th/U	Pb* (ppm)	$^{204}Pb/^{206}Pb$	f_{206} %	Radiogenic Ratios $^{206}Pb/^{238}U$	±	$^{207}Pb/^{235}U$	±	$^{207}Pb/^{206}Pb$	±	Ages (in Ma) $^{206}Pb/^{238}U$	±	$^{207}Pb/^{235}U$	±	$^{207}Pb/^{206}Pb$	±	Conc. %
1.1	263	420	1.597	125	0.000129	0.20	0.3530	0.0088	5.598	0.159	0.1150	0.0013	1949	42	1916	25	1880	20	104
2.1	235	323	1.373	102	0.000082	0.13	0.3324	0.0082	5.326	0.158	0.1162	0.0016	1850	40	1873	26	1899	25	97
3.1	130	143	1.103	56	0.000267	0.41	0.3569	0.0127	5.449	0.223	0.1107	0.0018	1967	61	1893	36	1812	30	109
4.1	192	304	1.579	92	0.000189	0.29	0.3555	0.0097	5.523	0.211	0.1127	0.0027	1961	46	1904	33	1843	43	106
5.1	179	200	1.119	79	0.000164	0.25	0.3691	0.0106	5.760	0.194	0.1132	0.0016	2025	50	1941	30	1851	26	109
6.1	195	369	1.899	97	0.000302	0.46	0.3533	0.0110	5.585	0.201	0.1147	0.0017	1950	52	1914	32	1874	27	104
7.1	141	267	1.887	72	0.000112	0.17	0.3589	0.0108	5.709	0.196	0.1154	0.0016	1977	51	1933	30	1886	25	105
8.1	575	596	1.037	99	0.001540	2.36	0.1244	0.0029	1.777	0.060	0.1036	0.0023	756	16	1037	22	1689	41	45
9.1	338	139	0.412	136	0.000187	0.29	0.3815	0.0098	6.000	0.182	0.1141	0.0015	2083	46	1976	27	1865	24	112
10.1	236	277	1.175	104	0.000508	0.78	0.3564	0.0098	5.479	0.184	0.1115	0.0018	1965	47	1897	29	1824	30	108
11.1	265	225	0.847	109	0.000164	0.25	0.3540	0.0257	5.513	0.415	0.1129	0.0015	1954	124	1903	67	1847	24	106
12.1	299	348	1.165	118	0.000746	1.19	0.3220	0.0075	4.853	0.211	0.1093	0.0037	1799	37	1794	37	1788	63	101
13.1	73	86	1.176	31	0.001588	2.54	0.3353	0.0153	5.300	0.523	0.1146	0.0094	1864	74	1869	88	1874	156	100
14.1	295	265	0.899	104	0.000275	0.44	0.3088	0.0054	4.961	0.141	0.1165	0.0024	1735	27	1813	24	1904	37	91
15.1	106	111	1.042	44	0.000781	1.25	0.3407	0.0107	5.239	0.314	0.1115	0.0053	1890	51	1859	52	1825	89	104
16.1	137	121	0.878	53	0.000622	0.99	0.3281	0.0096	5.214	0.297	0.1153	0.0052	1829	47	1855	50	1884	84	97
18.1	205	265	1.294	86	0.001038	1.66	0.3435	0.0109	5.283	0.279	0.1116	0.0043	1904	52	1866	46	1825	72	104
19.1	105	96	0.917	41	0.000451	0.72	0.3345	0.0071	5.100	0.162	0.1106	0.0023	1860	35	1836	27	1809	39	103
20.1	90	91	1.011	36	0.000318	0.51	0.3341	0.0110	5.019	0.205	0.1089	0.0022	1858	54	1823	35	1782	38	104
21.1	79	293	3.694	29	0.000477	0.76	0.2131	0.0063	2.377	0.156	0.0809	0.0045	1245	33	1236	48	1219	113	102
22.1	276	329	1.191	117	0.000236	0.38	0.3395	0.0066	5.363	0.126	0.1146	0.0013	1884	32	1879	20	1873	20	101
23.1	156	179	1.145	65	0.000505	0.81	0.3498	0.0077	5.549	0.174	0.1150	0.0023	1934	37	1908	27	1881	36	103
24.1	255	398	1.56	111	0.000128	0.21	0.3317	0.0070	5.253	0.127	0.1149	0.0011	1847	34	1861	21	1878	18	98
25.1	166	327	1.97	81	0.000469	0.75	0.3459	0.0082	5.190	0.172	0.1088	0.0022	1915	39	1851	29	1780	37	108

Notes :
1. Uncertainties given at the one σ level.
2. f_{206} % denotes the percentage of ^{206}Pb that is common Pb.
3. Correction for common Pb made using the measured $^{204}Pb/^{206}Pb$ ratio.
4. For % Conc., 100% denotes a concordant analysis.

Table 9. Summary of SHRIMP U-Pb zircon results for sample KPM3

Grain. spot	U (ppm)	Th (ppm)	Th/U	Pb* (ppm)	$^{204}Pb/^{206}Pb$	f_{206} %	Radiogenic Ratios $^{206}Pb/^{238}U$	±	$^{207}Pb/^{235}U$	±	$^{207}Pb/^{206}Pb$	±	Ages (in Ma) $^{206}Pb/^{238}U$	±	$^{207}Pb/^{235}U$	±	$^{207}Pb/^{206}Pb$	±	Conc. %
26.1	182	238	1.308	75	0.000105	0.17	0.3338	0.0072	5.303	0.144	0.1152	0.0017	1857	35	1869	24	1883	26	99
27.1	142	175	1.226	57	0.000229	0.37	0.3279	0.0093	5.059	0.186	0.1119	0.0023	1828	45	1829	32	1830	37	100
28.1	177	185	1.047	68	0.000351	0.56	0.3261	0.0078	5.069	0.175	0.1127	0.0025	1819	38	1831	30	1844	41	99
29.1	148	206	1.387	68	0.000174	0.28	0.3572	0.0068	5.691	0.138	0.1155	0.0015	1969	32	1930	21	1888	23	104
30.1	225	192	0.853	91	0.000203	0.32	0.3541	0.0067	5.414	0.142	0.1109	0.0018	1954	32	1887	23	1814	29	108
31.1	149	162	1.085	63	0.000202	0.32	0.3507	0.0064	5.409	0.143	0.1119	0.0019	1938	31	1886	23	1830	31	106
32.1	349	328	0.94	143	0.000122	0.20	0.3549	0.0069	5.533	0.137	0.1131	0.0015	1958	33	1906	21	1849	24	106
33.1	233	279	1.20	104	0.000001	0.00	0.3542	0.0093	5.728	0.167	0.1173	0.0012	1954	44	1936	26	1916	18	102
34.1	126	134	1.06	55	0.000108	0.17	0.3571	0.0111	5.620	0.206	0.1142	0.0018	1968	53	1919	32	1867	29	105
35.1	68	65	0.96	30	0.000376	0.58	0.3715	0.0121	5.645	0.250	0.1102	0.0029	2036	57	1923	39	1803	49	113
36.1	211	221	1.05	90	0.000113	0.17	0.3519	0.0091	5.521	0.169	0.1138	0.0015	1944	44	1904	27	1861	25	105
37.1	235	247	1.05	95	0.000073	0.11	0.3292	0.0083	5.147	0.160	0.1134	0.0018	1835	40	1844	27	1854	28	99
38.1	415	117	0.28	161	0.000038	0.06	0.3749	0.0089	6.276	0.159	0.1214	0.0008	2052	42	2015	22	1977	11	104
39.1	329	142	0.43	37	0.000498	0.87	0.1091	0.0030	0.846	0.052	0.0563	0.0029	667	17	623	29	463	118	144
40.1	128	136	1.07	57	0.000136	0.21	0.3631	0.0133	5.738	0.235	0.1146	0.0017	1997	63	1937	36	1874	26	107
41.1	121	153	1.27	53	0.000034	0.05	0.3448	0.0105	5.460	0.197	0.1149	0.0018	1910	51	1894	31	1878	29	102
42.1	170	211	1.24	76	0.000062	0.10	0.3563	0.0099	5.589	0.187	0.1138	0.0018	1965	47	1914	29	1861	28	106
43.1	275	325	1.18	112	0.000108	0.17	0.3149	0.0074	5.015	0.139	0.1155	0.0014	1765	36	1822	24	1888	22	94
44.1	97	105	1.08	42	0.000185	0.29	0.3525	0.0102	5.521	0.192	0.1136	0.0018	1947	49	1904	30	1858	29	105
45.1	110	195	1.77	53	0.000010	0.02	0.3460	0.0121	5.523	0.209	0.1158	0.0013	1916	58	1904	33	1892	20	101
46.1	277	312	1.13	116	0.000058	0.09	0.3394	0.0096	5.317	0.160	0.1136	0.0009	1884	46	1872	26	1858	14	101
47.1	272	249	0.91	110	0.000081	0.13	0.3398	0.0080	5.342	0.141	0.1140	0.0011	1886	39	1876	23	1864	17	101
48.1	143	156	1.09	57	0.000033	0.05	0.3244	0.0089	5.166	0.157	0.1155	0.0012	1811	43	1847	26	1888	19	96
49.1	64	26	0.41	13	0.000010	0.02	0.1968	0.0092	2.148	0.127	0.0792	0.0024	1158	50	1164	42	1176	62	99
50.1	93	120	1.29	41	0.000010	0.02	0.3466	0.0131	5.558	0.229	0.1163	0.0015	1918	63	1910	36	1900	23	101

Notes :
1. Uncertainties given at the one σ level.
2. f_{206} % denotes the percentage of ^{206}Pb that is common Pb.
3. Correction for common Pb made using the measured $^{204}Pb/^{206}Pb$ ratio.
4. For % Conc., 100% denotes a concordant analysis.

6. Discussion

a. Lower Roan Subgroup

Deposition of the Katanga Supergroup started at some time after 880 Ma. The ages of detrital zircons from the Lower Roan sediments indicate that their source region consisted mainly of Palaeoproterozoic rocks dated between 1790 and 2081 Ma (derived from the Palaeoproterozoic Lufubu Metamorphic Complex and Bangweulu Block magmatic arc terrane; Rainaud et al., 1999, 2004), with minor contributions from some younger Mesoproterozoic to early Neoproterozoic rocks (c. 1300 to 900 Ma), possibly derived from the Kibaran Belt (Cahen et al., 1984; Tack et al., 1999) and the Nchanga Granite.

The age spectrum of detrital zircons from the Lower Roan Subgroup does not show any older Palaeoproterozoic to Mesoarchaean (c. 2.2 to 3.2 Ga) ages, such as those obtained from detrital zircons in the Muva quartzite south of Mufulira (Rainaud et al., 2003). This indicates that the Roan sediments were not derived from the same sources as the Muva quartzites (which are interpreted to have formed as a molasse to the Kibaran orogeny, deriving components from the Congo Craton; Rainaud et al., 2004). At the time of Roan sedimentation, the Congo Craton west of the Kibaran belt was covered by the Mbuji-Mayi (Bushimay) succession (Raucq, 1970), which is older than 950 Ma (Cahen et al., 1984), thus the Archaean and early Palaeoproterozoic rocks of the Congo Craton may not have outcropped to provide detritus into the Katangan basin. The lack of recycled detrital Archaean and older Palaeoproterozoic zircons derived from the Muva sedimentary rocks also indicates the relative unimportance of the Muva quartzites in the provenance of the Roan sediments. The Muva sedimentary rocks in the Copperbelt region must have been present only as a thin veneer over the Palaeoproterozoic magmatic arc rocks of the Lufubu Metamorphic Complex, which provided the bulk of the detritus for the Roan sediments. Quartzite pebbles and boulders in the Roan-Muliashi Basin (Lee-Potter, 1961;

Mendelsohn, 1961b), the Chambishi-Nkana Basin (Garlick, 1961; Jordaan, 1961) and Nchanga (McKinnon and Smit, 1961), together with some polycrystalline quartzite clasts recorded from Lower Roan aeolian quartzites at Musoshi Mine (Master, 1993) may have been derived from erosion of the thin veneer of Muva quartzites. By comparison with the diamictites of the Grand Conglomerat, which have a clast population dominated by quartzites (see below), the relative sparsity of quartzite pebbles in the Roan sediments indicates that the source region, formerly covered by a veneer of Muva quartzite, had been uplifted and eroded, exposing the Palaeoproterozoic basement which dominated the sediment supply. This would be consistent with active faulting in the provenance area, and supports models for the deposition of the Roan Group in an active continental rift (e.g., Porada, 1989; Master, 1993; Tembo et al., 1999).

b. Nguba Group- Grand Conglomerat Formation

The petrography of the Grand Conglomerat at Kipushi indicates that it contains numerous clasts derived from a mixed plutonic (granitic and amphibolitic) and metavolcanic (quartz porphyry schist) terrain. The presence of abundant monocrystalline euhedral to subhedral quartz crystals, some attached to crenulated biotite schist, indicates an origin from metamorphosed volcanic quartz porphyries, such as those in the Lufubu Metamorphic Complex (Rainaud et al., 2004). It should, however, be noted that the composition of the clasts in the Grand Conglomerat at Kipushi is different from the usual assemblage of clasts found in the Grand Conglomerat elsewhere within the Lufilian Arc, which is dominated by the presence of quartzite pebbles derived from the Kibaran Belt or from the Muva Supergroup, occurring together with less abundant clasts of granitic and basic rocks (François, 1973; Cahen, 1978). Recent observations by the senior author from outcrops at Shituru (Ngoie, 2003); S of Luiswishi (Cailteux et al., 2003b); NW of Kakanda and SE of Fungurume (Mbuyi, 2003) confirm the presence of abundant rounded and faceted quartzite clasts in the Grand Conglomerat in these areas.

In glacial tillites, distinctive clasts whose origin is pinpointed exactly are known as glacial indicators (Norman Smith, pers. comm., 1998). The Grand Conglomerat intersected by surface borehole CK73 drilled in Zambia close to Kipushi Mine contains exotic granitic clasts. One of these clasts is a white porphyritic granitoid, containing large (up to 1 cm long) white euhedral feldspar phenocrysts. This granitoid variety is completely unknown on the Copperbelt in Zambia (Pier Binda, pers. comm., 1993), but is known to outcrop on the Luina Dome in the Democratic Republic of Congo, close to the Zambian Border (Gysin, 1933, 1935; Leon de Jonghe, pers. comm., 1993). In borehole KHI 1150/34/HZ-S at Kipushi Mine, a 15 cm long boulder of a porphyritic biotitic granitoid with large white euhedral feldspar phenocrysts, up to 2.3 cm long, was intersected in the Grand Conglomerat at a depth of 194.75 m. (Figure 12) The distinctive feldspar-porphyritic granitoid clasts in the Grand Conglomerat of the Kipushi district are thus glacial indicators, and point to apparent west-northwesterly glacial transport for a distance of about 100 km, from the Luina Dome towards Kipushi. Restoring the ca. 150 km maximum northward translation of the strata at Kipushi during the thrusting of the Lufilian Orogeny (Jackson et al., 2003) would yield a glacial transport vector for the Grand Conglomerat trending roughly 150 km west-southwesterly from the Luina Dome. It is also possible that the porphyritic granitoids found in the Grand Conglomerat of the Kipushi district may have been derived from some unknown porphyritic intrusions, similar in composition and age to the intrusions of the Luina Dome, but farther to the west, which are now buried under the thick pile of Katangan thrust sheets.

Figure 12. Photograph of a feldspar-porphyritic granitoid clast in the Grand Conglomerat from Kipushi Mine, D. R. Congo.

The ages of zircons from the Grand Conglomerat at Kipushi indicate a provenance from the Palaeoproterozoic Ubendian basement, as well as from Kibaran granite sources and Neoprotrozoic sources. The age of the youngest detrital zircon would set an upper limit for the age of the Grand Conglomerat. In the present study, the youngest zircon is only 88% concordant, and gives an imprecise age of 729 ± 50 Ma. This is consistent with the age of the Grand Conglomerat being less than 760 ± 5 Ma (see above).

Porphyritic granitoids of the Luina Dome have been dated at 1882 +23/-19 Ma (Ngoyi et al., 1991). These granitoids from the Luina Dome, or the younger Lufubu Schists from Kinsenda Mine on the flanks of the Luina Dome (which have an age of 1873 ± 8 Ma; Rainaud et al., 2004), could be the source of the detrital zircons in the Grand Conglomerat having ages of 1846 ± 22 Ma and 1866 ± 18 Ma. Thus the age of detrital zircons, as well as distinctive porphyritic granite and metavolcanic quartz porphyry clasts, indicate that the Grand Conglomerat near Kipushi had a source region near the Luina Dome, in a restored pre-tectonic position about 150 to the ENE. This indicates that during deposition of the Grand Conglomerat, the Palaeoproterozoic rocks around the Luina Dome, at the northern end of the Kafue Anticline, were exposed on the surface as a basement high, just as they were during Roan Group deposition, since pebbles derived from the

Luina and Konkola Domes are abundant in Lower Roan conglomerates at Musoshi, Kinsenda and Konkola mines. Sedimentological evidence thus indicates that the Kafue Anticline was a basement high during both Roan and Nguba (ex-Lower Kundelungu) Group deposition, and did not originate entirely as an anticlinal fold above a basement-involved frontal ramp during thick-skinned thrusting associated with the Lufilian Orogeny, as was proposed by Daly et al. (1984).

The oldest Palaeoproterozoic detrital zircon age of 1945 ± 15 Ma from the Grand Conglomerat could be derived from units similar to the Samba Porphyry and associated metavolcanics, which have an age of 1964 ± 12 Ma (Rainaud et al., 2004). The younger group of detrital zircons, of late Mesoproterozoic to Neoproterozoic age could be derived from granitoids of the Kibaran Belt, which have ages ranging down to 1 Ga (Cahen et al., 1984; Kokonyangi et al., 2002), and from granites associated with a phase of magmatic activity preceding Katangan deposition (e.g., the 880 Ma Nchanga Granite, Armstrong et al., 2004), or the c. 843 Ma Lusaka Granite (Barr et al., 1978), or the 820 ± 7 Ma Ngoma gneiss (Hanson et al., 1988, 1994).

Because the Grand Conglomerat from Kipushi appears to have a different clast population from the rest of the Grand Conglomerat outcrops in the Lufilian arc, the ages of detrital zircons from the Kipushi area may not be fully representative of the provenance. For example, the quartzite pebbles that are so abundant in the Grand Conglomerat regionally, seem to be absent from the Kipushi diamictites, and so are any recycled older Palaeoproterozoic to Archaean zircons (c. 2.2 Ga to 3.2 Ga) which are present in Muva quartzite from the Zambian Copperbelt (Rainaud et al., 2003). Thus we suspect that if a similar study of detrital zircons were undertaken on samples of the Grand Conglomerat where it is typically dominated by quartzite clasts, then older recycled zircons derived from these quartzites will be found.

According to Key et al. (2001), the ages of the volcanic units in the Nguba Group bracket the age of the Grand Conglomerat between 760 ± 5 and 735 ± 5 Ma. However, as noted above, the stratigraphic position of the younger volcanic unit is in doubt. Thus the Grand Conglomerat can only definitely be given a maximum age of 760 ± 5 Ma. This allows only a broad correlation of the Grand Conglomerat with other Neoproterozoic glacial diamictite units such as the Chuos diamictite in the Damara Orogen, Namibia (Hoffmann & Prave, 1996), diamictites in the Gariep and Saldania Belts, South Africa (Fölling & Frimmel, 2002) and the ca. 750-700 Ma Sturtian diamictites of the Adelaidean Supergroup, South Australia (Kaufman et al., 1997; Evans, 2000). If these various Neoproterozoic glaciations are part of a global "snowball earth" Sturtian glaciation, then they are all probably around 710 Ma in age, which is the age of two accurately dated Sturtian glacial diamictites, the Scout Mountain Member of the Pocatello Formation, Idaho, and the Gubrah Member in Oman (Fanning and Link, 2003; Hoffman et al., 2004). However, they may also be diachronous, spanning about 50 Ma from c. 750 to c. 700 Ma (Fanning and Link, 2003).

c. Kundelungu Group- Petit Conglomerat Formation

Our petrographic studies of the Petit Conglomerat are confined to samples from Kipushi Mine, taken from borehole KHI 1150PVSSW, at depths between 55.21 and 75.00 m. Here the Petit Conglomerat is 24.1 m thick, and consists of a fine-grained biotitic siltstone with a few scattered clasts, about 0.5 mm across, ranging up to a maximum size of 5 mm. The clasts consist of quartz (both mono- and polycrystalline), carbonate, shale, chert, and altered orthoclase. These clasts are mainly of intrabasinal derivation, with some contribution from basement granitoids (orthoclase). The presence in this rock of acritarchs (of planktonic origin), similar to acritarchs described from Kundelundu beds by Hacquaert (1931a,b,c) and Choubert (1932), indicates that the rock was deposited in glaciomarine conditions, rather than in a continental moraine. This fine-grained gritty siltstone facies of the Petit Conglomerat is a further indication of the general southward decrease in pebble size that has been recorded in the Petit Conglomerat, which contains much larger and more abundant pebbles in the north (Cahen, 1978), where it is also a lot thicker (up to 80 m in the Lukafu area, Vanden Brande, 1936). Cahen (1978) distinguished two facies in the Petit Conglomerat: a southern diamictite facies with small (<2 cm) clasts, and a northern mixed diamictite and conglomerate facies, with large clasts (up to 1 m granite clasts described by Grosemans, 1935) of varied compositions: quartz, granites, basic rocks, agates, amygdaloidal lavas, rhyolites, quartzites, siliceous oolites, sandstones and shales; among these, many faceted and striated clasts were observed (Grosemans, 1935; Vanden Brande, 1936; Batumike et al., 2002). Many of the clasts originated from the adjacent Kibaran Belt to the northeast, and from the Kibambale volcanic complex to the north (Dumont and Cahen, 1978). In the Kapulo area of NE Katanga (28°40'-29°40'E, 7°55'-8°10'S), just north of Lake Mweru, a distinctive and heterogeneous suite of clast types (up to a maximum diameter of 30 cm) have been recorded from the Petit Conglomerat diamictite- these include quartzite, rhyolite, porphyries, alaskites, and rare clasts of gneiss, mica schists, metaconglomerates, and pisolitic black cherts (Andre, 1976; Cahen, 1978). In this case, the clasts are clearly derived from the adjacent Bangweulu Block to the east: rhyolites and porphyries from the Marungu or Luapula porphyries (Abraham, 1959; Thieme, 1971, Kabengele et al., 1987); alaskites from Kapulo (André, 1976); quartzites and metaconglomerates from the Mporokoso Group (Andersen and Unrug, 1984). Recent petrographic and geochemical studies on the Petit Conglomerat and other sedimentary rocks of the Nguba Group (Batumike et al., 2002, 2003) support the north-south facies variations, and a derivation from the Kibaran Belt and Bangweulu Block to the northwest and northeast of the Katangan basin,

From the available radiometric data, the age of the Petit Conglomerat is not yet well constrained, and is only bracketed between 735 ± 5 Ma, the age of volcanics in the West Lunga Formation in the Nguba Group (Liyungu et al., 2001), and c. 620 Ma, the age of uraninites from veins in thrust zones that affect the Katangan stratigraphy to the top of the Kundelungu Group (Cahen, 1973). The Petit Conglomerat and its overlying cap carbonate, the Calcaire Rose, may be correlated with the Ghaub diamictite and Rasthof cap carbonate in the Otavi Group of the Damara Orogen, Namibia, which are dated at 635.5 ± 1.2 Ma (Hoffman et al., 2004).

d. Biano Group

Detrital muscovites from the red siltstones of the Biano Group show a spread of laser $^{40}Ar/^{39}Ar$ ages over 900 Ma (between 1478 and 573 Ma) indicating that these muscovite grains have not been reset since sedimentation, but that they retain the primary ages derived from their parent rocks. The youngest detrital muscovite age of 573 ± 5 Ma is regarded as the maximum age for the sediments of the Biano Group, which are thus constrained to be terminal Neoproterozoic and/or early Palaeozoic in age, and this timing strongly supports models which regard the Biano Group as being deposited in a foreland basin to the Pan-African Lufilian orogeny (e.g., Wendorff, 2001a,b, 2002b, 2003a), rather than the earlier models which regarded it as having been deposited in an aulacogen (e.g., Porada, 1989). Furthermore, the Biano Group has two main ages of detrital zircons. The older ages (1977 ± 11 – 1780 ± 37 Ma) span the age range of magmatic arc rocks of the Bangweulu Block, including the basement in the Copperbelt (Brewer et al., 1979; Ngoyi et al., 1991; Rainaud et al., 2004). The younger ages (1219 ± 113 and 1176 ± 62 Ma) overlap with the 1134 ± 8 Ma age of the Lusenga hornblende syenite, which intrudes the Mporokoso Group on the Bangweulu Block (Brewer et al., 1979; Andersen & Unrug, 1984). The Biano Group thus appears to have been derived from a source terrain comprising the Bangweulu Block (consistent with the measured palaeocurrent directions), and from a terrain (the Lufilian arc) which had undergone metamorphism from 638 to 573 Ma. Thus these sediments are likely to have been deposited in a foreland basin ahead of the Lufilian orogenic front, having been derived from erosion of the orogen itself, as well as from the forebulge surrounding the foreland basin (the Bangweulu Block).

7. Conclusions

The new SHRIMP U-Pb data on the ages of detrital zircons from sedimentary rocks of the Neoproterozoic Katanga Supergroup, and the preliminary ^{40}Ar-^{39}Ar data on detrital muscovites from the uppermost Katangan beds, give information on the age and likely nature of the source regions for the Katangan sediments and provide age constraints on upper Katangan (Biano Group) sedimentation.

Detrital zircon ages indicate a mainly Palaeoproterozoic (between 2081 ± 28 and 1836 ± 26 Ma) provenance for the Katanga basin, derived from the Metamorphic Lufubu Complex of the Kafue Anticline and the Bangweulu Block to the north of the outcrop belt. Detrital zircons and clasts from Roan Group sediments indicate a source from the Palaeoproterozoic granitoids of the Kafue Anticline, as well as, more locally, from the Nchanga Granite. The relative scarcity of Muva quartzite clasts, as well as the total absence of any >2.2 Ga older Palaeoproterozoic and Archaean recycled zircons (that are known to be abundant in the Muva), indicate the relative unimportance of the Muva quartzites in the provenance of the Roan Group, which was derived mainly from a block-faulted Palaeoproterozoic basement region from which a relatively thin veneer of Muva quartzites had been stripped away by erosion.

Detrital zircons and clasts from the Grand Conglomerat glacial diamictite in the Kipushi area indicate a source from the Palaeoproterozoic metavolcanic porphyries and granitoids of the Luina Dome region, near the western end of the Kafue Anticline, which was a basement high during Nguba Group deposition. Elsewhere in the Lufilian Arc, the Grand Conglomerat contains abundant quartzite clasts, which were derived either from the Kibaran Belt, or from a cover of Muva Supergroup rocks to the north of the Katangan depository. Minor zircons of Mesoproterozoic age may have been derived from granitoids of the Kibaran belt. The size distribution and nature of clasts in the Petit Conglomerat indicate a north-to-south transport direction, corresponding to the diminution in size and abundance of extrabasinal clasts (derived from the Kibaran Belt and the Bangweulu Block). Finally, $^{40}Ar/^{39}Ar$ age data from detrital muscovites from Biano Group siltstones give a maximum age of sedimentation of 573 ± 5 Ma, strongly supporting previous models that the Biano Group was deposited in a foreland basin of the Lufilian Orogen. The ages of detrital zircons in the Biano Group indicate a provenance from the basement plutonic granitoids, as well as from younger intrusive complexes, of the Bangweulu Block, which were exposed in the forebulge flanking the Katangan foreland basin.

ACKNOWLEDGEMENTS

We are grateful to Anglovaal (Zambia) and Claus Schlegel for supporting this study and for permission to publish this data. We thank ZCCM and KCM (Zambia), Gécamines and SODIMICO (D. R. Congo) for access to drillcore. SM is grateful to Prof. M. Kabengele and Flungu Musendu for logistical support on the Kundelungu Plateau. Prof. K.A. Eriksson is thanked for a thorough and helpful review of this paper.

8. References

Abraham, D. (1959). *The stratigraphical and structural relationship of the Kundelungu System, Plateau Series and basement rocks in the Mid-Luapula valley, Northern Rhodesia*. D. Phil. Thesis, Univ. Leeds, 152 pp.

Andersen, L.S., Unrug, R. (1984). Geodynamic evolution of the Bangweulu Block, northern Zambia. Precambrian Res., 25, 187-212.

André, L. (1976). *Etude aérophotomorphologiques et pétrographique du Katangien de la mosaïque contrôlée de Kapulo au Shaba*. Mémoire de licence, Univ. Libre de Bruxelles, Belgique.

Armstrong, R.A. (2000). Ion microprobe (SHRIMP) dating of zircons from granites, granulites and volcanic samples from Zambia. Unpubl. Rep., ANU, PRISE Job No. A99-160, Canberra.

Armstrong, R.A., Master, S., Robb, L.J., Lobo-Guerrero, A. (2004). Geochronology of the Nchanga Granite, and constraints on the maximum age of the Katanga Supergroup, Zambian Copperbelt. J. Afr. Earth Sci. (this issue).

Barr, M.W.C., Cahen, L., Ledent, D. (1978). Geochronology of syntectonic granites from central Zambia: Lusaka Granite and granite NE of Rufunsa. Ann. Soc. géol. Belg., 100, 47-54.

Barron, J.W., Broughton, D.W., Armstrong, R.A., Hitzman, M.W. (2003). Petrology, geochemistry and age of gabbroic bodies in the Solwezi area, northwestern Zambia. In: Contributions presented at the 3rd IGCP-450 Conference, Proterozoic Sediment-hosted Base Metal Deposits of Western Gondwana; Conference and Field Workshop Lubumbashi 2003, Lubumbashi, D.R. Congo, 75-77.

Batumike, M.J., Cailteux, J.L.H., Kampunzu, A.B. (2002). Nguba and Kundelungu Groups, Katangan Belt (Congo): Lithostratigraphy and petrography. Extended Abstracts, 11th Quadrennial IAGOD Symposium and Geocongress 2002, 22-26 July 2002, Windhoek, Namibia, CD-ROM.

Batumike, M.J., Roser, B.P., Kampunzu, A.B., Cailteux, J.L.H. (2003). Geochemical investigations of Nguba and kundelungu Groups, Katangan Supergroup (Congo): Provenance and tectonic setting. In: Contributions presented at the 3rd IGCP-450 Conference, Proterozoic Sediment-hosted Base Metal Deposits of Western Gondwana; Conference and Field Workshop Lubumbashi 2003, Lubumbashi, D.R. Congo, 89-93.

Benn, D.I., Evans, D.J.A. (1998). *Glaciers & Glaciation*. Arnold, London, 734 pp.

Binda, P.L. (1972). Zircons of the Nchanga Granite and overlying metasediments, Zambia. 24th Int. Geol. Congr., Montreal, Sect. 1, Precambrian Geology, 179-186.

Binda, P.L., van Eden, J.G. (1974). Sedimentological evidence on the origin of the Precambrian Great Conglomerate (Kundelungu Tillite), Zambia. Paleogeogr. Paleoclimatol. Paleoecol., 12, 151-168.

Brewer, M.S., Haslam, H.W., Darbyshire, D.P.F., Davis, A.E. (1979). Rb-Sr age determinations in the Bangweulu Block, Luapula Province, Zambia. Institute of Geological Sciences, London, Report 79/5, 1-11.

Cahen, L. (1963). Glaciations anciennes et dérive des continents. Ann. Soc. géol. Belg., 86(1), B19-B84.

Cahen, L. (1973). L'uraninite de 620 m.a. post-date tout le Katangien, mise au point. Mus. roy. Afr. centr., Dept. Géol. Minér., Rapp. Ann. 1972, 35-38.

Cahen, L. (1978). Les mixtites anté-cambriennes de l'est du Zaïre: Mise au point intérimaire. Mus. roy. Afr. centr., Tervuren, Dépt. Géol. Min., Rapp. Ann. 1977, 33-64.

Cahen, L., Delhal, J., Ledent, D. (1970). On the age and petrogenesis of the microcline-bearing pegmatite veins at Roan Antelope and at Musoshi

(Copperbelt of Zambia and S-E Katanga). Ann. Mus. roy. Afr. Centr., Sci. géol., 65, 43-68.

Cahen, L., Snelling, N.J., Delhal, J., Vail, J.R., Bonhomme, M., Ledent, D. (1984). *The Geochronology and Evolution of Africa*. Clarendon Press, Oxford, 512 pp.

Cailteux, J.L.H. (2003). Comment from the Organizer. In: Guide-Book to the Field Trip, IGCP No. 450, Proterozoic Sediment-hosted Base Metal Deposits of Western Gondwana; Conference and Field Workshop Lubumbashi 2003, Lubumbashi, D.R. Congo, 204-205.

Cailteux, J., Binda, P.L., Katekesha, W.M., Kampunzu, A.B., Intiomale, M.M., Kapenda, D., Kaunda, C., Ngongo, K., Tshiauka, T., Wendorff, M. (1994). Lithostratigraphical correlation of the Neoproterozoic Roan Supergroup from Shaba (Zaire) and Zambia, in the Central African copper-cobalt metallogenic province. In: Kampunzu, A.B., Lubala, R.T. (Eds.), Neoproterozoic belts of Zambia, Zaire and Namibia (Special Issue), J. Afr. Earth Sci., 19(4), 265-278.

Cailteux, J.L.H., Kampunzu, A.B., Ngoie Bwanga, F. (2003a). Lithostratigraphy of the Mwashya Subgroup in Congo (Central African Copperbelt), with special reference to the Luiswishi area. In: Contributions presented at the 3rd IGCP-450 Conference, Proterozoic Sediment-hosted Base Metal Deposits of Western Gondwana; Conference and Field Workshop Lubumbashi 2003, Lubumbashi, D.R. Congo, 83-87.

Cailteux, J.L.H., Kankomba, R., Batumike, J., Mazau, J. (2003b). The Luiswishi stratiform Cu-Co deposit and geological context. In: Guide-Book to the Field Trip, IGCP No. 450, Proterozoic Sediment-hosted Base Metal Deposits of Western Gondwana; Conference and Field Workshop Lubumbashi 2003, Lubumbashi, D.R. Congo, 207-209.

Choubert, B. (1932). Nouvelles recherches sur les algues du niveau du "Calcaire rose oolithique" du Kundelungu supérieur du Congo belge (Province Orientale du Katanga). *Bulletin de la Société Belge de Géologie, Paléontologie et Hydrogéologie*, **42**, 63-70.

Claoué-Long, J. C., Compston, W., Roberts, J., Fanning, C. M. (1995). Two carboniferous ages: a comparison of SHRIMP zircon dating with conventional zircon ages and ^{40}Ar-^{39}Ar analysis. In: Berggren, W. A., Kent, D. V., Aubry, M. P., Hardenbol, J. (Eds.), *Geochronology Time Scales and Global Stratigraphic Correlation*. SEPM Special Publication, 54, pp. 1-21

Daly, M.C., Chakraborty, S.K., Kasolo, P., Musiwa, M., Mumba, P., Naidu, B., Namateba, C., Ng'ambi, O., Coward, M.P. (1984). The Lufilian arc and Irumide belt of Zambia: results of a traverse across their intersection. J. Afr. Earth Sci., 4, 311-318.

Dumont, P., Cahen, L. (1978). Les complexes conglomératique de la bordure sud-orientale de la chaïne kibarienne et leurs relations avec les couches katangiennes de l'arc lufilien. Mus. Roy. Afr. Centr., Tervuren, Dépt. Géol. Min., Rapp. Ann. 1977, 111-135.

Evans, D.A.D. (2000). Stratigraphic, geochronological, and paleomagnetic constraints upon the Neoproterozoic climatic paradox. American Journal of Science, 300, 347-433.

Fanning, C.M., Link, P.K. (2003). 700 Ma U-Pb SHRIMP age for Sturtian (!) diamictites of the Pocatello Formation, Southeastern Idaho. Geological Society of America Abstracts with Programs, 33(6), September 2003, p. 389.

Fleischer, V.D., Garlick, W.G., Haldane, R. (1976). Geology of the Zambian Copper Belt. In: Wolf, K.H. (Ed.) Handbook of Strata-bound and Stratiform Ore Deposits, Vol. 6. Elsevier, New York, pp. 223-352.

Fölling, P.G., Frimmel, H.E. (2002). Chemostratigraphic correlation of carbonate successions in the Gariep and Saldania Belts, Namibia and South Africa. Basin Research, 14, 69-88.

François, A. (1973). L'extrémité occidentale de l'arc cuprifère shabien. Étude géologique. Dépt. géol. Gécamines, Likasi, Shaba, Zaire, pp. 120.

François, A. (1995). Problèmes relatifs au Katanguien du Shaba. In: Wendorff, M., Tack, L. (Eds.), Late Proterozoic Belts in Central and Southwestern Africa. IGCP Project 302. Ann. Musée Royal de l'Afrique Centrale, Tervuren, Belgique, Sci. Géol., 101, pp. 1-20.

Garlick, W.G. (1961). Chambishi. In: Mendelsohn, F. (Ed.), *The Geology of the Northern Rhodesian Copperbelt*. Macdonald, London, 281-297.

Garlick, W.G. (1973). The Nchanga granite. In: Lister, L.A. (Ed.), Symposium on Granites, Gneisses and Related Rocks. Geol. Soc. S. Afr. Spec. Publ., 3, pp. 455-474.

Garlick, W.G., Brummer, J.J. (1951). The age of the granites of the Northern Rhodesian Copperbelt. Econ. Geol., 46, 478-497.

Grosemans, P. (1935). Contribution à l'etude du conglomérat de base (petit conglomérat) du Kundelungu supérieur. Ann. Serv. Mines Comité Spécial du Katanga, 5, 38-57.

Gysin, M. (1933). Recherches géologiques et pétrographiques dans le Katanga méridional. Mém. Inst. roy. Col. belge, Sc. Nat. et Méd., 6(1), 259 pp.

Gysin, M. (1935). Essai de classification des granites du Katanga méridional d'après l'étude planimétrique des coupes minces. C. R. Séances de la Soc. Phys. et Hist. Nat., Genève, 52, 243-246.

Hacquaert, A.L. (1931a). Ontdekking van fossiele Groenwieren in het Calcaire rose (Kundelungu-systeem) van Katanga. Natuurwetenschaplijke Tijdschrift, 13(3-5), 131-136.

Hacquaert, A.L. (1931b). Nieuwe fossielen uit een kalksteen van het Kundelungu-systeem van Katanga (Belgisch-Congo). Natuurwetenschaplijke Tijdschrift., 13, 281-284.

Hacquaert, A.L. (1931c). Présentation de fossiles découverts au Katanga dans le Calcaire rose (système du Kundelungu) au Katanga. Bull. Soc. belge Géol. Paléontol. Hydrol., 41, 117-119.

Hanson, R.E., Wilson, T.J., Munyanyiwa, H. (1994). Geologic evolution of the Neoproterozoic Zambezi Orogenic Belt in Zambia. J. Afr. Earth Sci., 18, 135-150.

Hanson, R.E., Wilson, T.J., Wardlaw, M.S. (1988). Deformed batholiths in the Pan-African Zambezi Belt, Zambia: Age and implications for regional Proterozoic tectonics. Geology, 16, 1134-1137.

Hoffman, P.F., Kaufman, A.J., Halverson, G.P. and Schrag, D.P. (1998). A Neoproterozoic snowball earth. Science, 281, 1342-1346.

Hoffmann, K.-H., Condon, D.J., Bowring, S.A., Crowley, J.L. (2004). U-Pb zircon dates for the Neoproterozoic Ghaub Formation, Namibia: constraints on Marinoan glaciation. Geology, 32(9), 817-820.

Hoffmann, K.-H., Prave, A.R. (1996). A preliminary note on a revised subdivision and regional correlation of the Otavi Group based on glaciogenic diamictites and associated cap dolostones. Communications Geological Survey Namibia, 11, 77-82.

Jackson, M.P.A., Warin, O.N., Woad, G.M., Hudec, M.R. (2003). Neoproterozoic allochthonous salt tectonics during the Lufilian orogeny in the Katangan Copperbelt, central Africa. Geol. Soc. America Bulletin, 115(3), 314-330.

Jordaan, J. (1961). Nkana. In: Mendelsohn, F. (Ed.), *The Geology of the Northern Rhodesian Copperbelt*. Macdonald, London, 297-328.

Kabengele, M., Lubala, R.T., Cabanis, B. (1987). Le magmatisme du plateau des Marungu (secteur de Pepa-Lubumba, nord-est du Shaba, Zaïre)- Caractéristiques pétrologiques et géochimiques- Signification géodynamique dans l'évolution de la chaîne Ubendienne. In: Matheis, G., Schandelmeier, M. (Eds.) *Current Research in African Earth Sciences*. Balkema, Rotterdam, 13-16.

Kabengele, M., Mashala, T., Loris, N.B.T. (2003). Geochemistry of the Lower Mwashya pyroclastic rocks in the Likasi-Kambove area (D.R. Congo). In: Contributions presented at the 3rd IGCP-450 Conference, Proterozoic Sediment-hosted Base Metal Deposits of Western Gondwana; Conference and Field Workshop Lubumbashi 2003, Lubumbashi, D.R. Congo, 69-74.

Kaufman, A.J., Knoll, A.H., Narbonne, G.M. (1997). Isotopes, ice ages, and terminal Proterozoic earth history. Proc. Natl. Acad. Sci., USA, 94, 6600-6605.

Key, R., Banda, J. (2000). The Geology of the Kalene Hills area. Rep. Geol. Surv. Zambia, 107 pp.

Key, R. M., Liyungu, A. K., Njamu, F. M., Somwe, V., Banda, J., Mosley, P. N., Armstrong, R. A. (2001). The Western arm of the Lufilian Arc, NW Zambia and its potential for copper mineralization. J. Afr. Earth Sci., 33 (3-4), 503-528.

Kokonyangi, J., Armstrong, R., Kampunzu, A.B., Yoshida, M., Okudaira, T. (2003). Magmatic evolution of the Kibarides Belt (Katanga, Congo) and implications for Rodinia reconstruction: field observations, U-Pb SHRIMP geochronology and geochemistry of granites. Extended Abstracts, 11th Quadrennial IAGOD Symposium and Geocongress 2002, 22-26 July 2002, Windhoek, Namibia, CD-ROM.

Lee-Potter, J.B. (1961). Baluba. In: Mendelsohn, F. (Ed.), *The Geology of the Northern Rhodesian Copperbelt*. Macdonald, London, 343-351.

Lefebvre, J.J. (1973). Présence d'une sédimentation pyroclastique dans le Mwashya inférieur du Shaba méridional (ex-Katanga). Ann. Soc. Géol. Belg., 96, 197-218.

Lefebvre, J.J. (1974). Mineralisations cupro-cobaltiferes associées aux horizons pyroclastiques situés dans le faisceau supérieur de la Serie de Roan, à Shituru, Shaba, Zaire. In: Bartholomé, P. et al. (Eds.), Gisements stratiformes et provinces cuprifères. Soc. Géol. Belgique, Liège, 103-122.

Lefebvre, J.J. (1975). Les roches ignées dans le Katangien du Shaba (Zaïre). Le district du cuivre. Annales de la Société Géologique de Belgique, 98, 47–73.

Liyungu, A. K., Mosley, P.N., Njamu, F.M., Banda, J. (2001). Geology of the Mwinilunga area. Rep. Geol. Surv. Zambia, 110, 36 pp.

Ludwig, K.R. (2000). *Users Manual for Isoplot/Ex version 2.3, a geochronological toolkit for Microsoft Excel*. Berkeley Geochronology Center, Special Publications, 1a.

McDougall, I., Harrison, T. M. (1999). *Geochronology and thermochronology by the ^{40}Ar-^{39}Ar method*. Second Edition. Oxford University Press, New York. 288 pp.

Master, S. (1993). Preliminary observations on the sedimentology of the Roan Group at Musoshi (Zaire) and Konkola (Zambia), with implications for Katangan stratigraphy. Abstracts, IGCP Project 302: The structure and metallogenesis of Central African Late Proterozoic Belts, Copperbelt Field Conference, Kalulushi, Zambia, 23-31 July 1993.

Mbuyi, F. (2003). A folded Nguba-Kundelungu section. In: Guide-Book to the Field Trip, IGCP No. 450, Proterozoic Sediment-hosted Base Metal Deposits of Western Gondwana; Conference and Field Workshop Lubumbashi 2003, Lubumbashi, D.R. Congo, 218-219.

McKinnon, D.M., Smit, N.J. (1961). Nchanga. In: Mendelsohn, F. (Ed.), *The Geology of the Northern Rhodesian Copperbelt*. Macdonald, London, 234-275.

Mendelsohn, F. (Ed.) (1961a). *The Geology of the Northern Rhodesian Copperbelt*. Macdonald, London, 523 pp.

Mendelsohn, F. (1961b). Roan Antelope. In: Mendelsohn, F. (Ed.), *The Geology of the Northern Rhodesian Copperbelt*. Macdonald, London, 351-405.

Museu, M. (1987). Considérations sur l'origine du Grand Conglomérat de base du Kundelungu inférieur au Shaba (République du Zaïre). Mus. roy. Afr. centr., Tervuren (Belg.), Dépt. Géol. Min., Rapp. Ann 1985-1986, pp. 165-168.

Ngoie, F.B. (2003). The Mwashya Subgroup at Shituru. In: Guide-Book to the Field Trip, IGCP No. 450, Proterozoic Sediment-hosted Base Metal Deposits of Western Gondwana; Conference and Field Workshop Lubumbashi 2003, Lubumbashi, D.R. Congo, 214-215.

Ngoyi, K., Liégeois, J.-P., Demaiffe, D., Dumont, P. (1991). Age tardi-ubendien (Protérozoïque inférieur) des dômes granitiques de l'arc cuprifère zaïro-zambien. C. R. Acad. Sci., Paris, 313, Sér. II, 83-89.

Porada, H. (1989). Pan-African rifting and orogenesis in Southern to Equatorial Africa and Eastern Brazil. Precambrian Res., 44, 103-136.

Rainaud, C., Armstrong, R.A., Master, S., Robb, L.J. (1999). A fertile Palaeoproterozoic magmatic arc beneath the Central African Copperbelt. In: Stanley, C.J. et al. (Eds.), *Mineral Deposits: Processes to Processing, Volume 2*. A.A. Balkema, Rotterdam, 1427-1430.

Rainaud, C., Master, S., Armstrong, R.A., Robb, L.J., Mumba, P.A.C.C. (2004). Nature and geochronology of the Palaeoproterozoic basement in the Central African Copperbelt. J. Afr. Earth Sci. (this issue).

Rainaud, C., Master, S., Armstrong, R.A., Robb. L.J. (2003). A cryptic Mesoarchaean terrane in the basement to the Central African Copperbelt. Journal of the Geological Society, London, 160, 11-14.

Raucq, P. (1970). Nouvelles acquisitions sur le système de la Bushimay, République Démocratique du Congo. *Annales du Musée Royal de l'Afrique Centrale, Sci. Géol*., 69, 156 pp.

Robert, M. (1956). *Géologie et géographie du Katanga y compris l'étude des ressources et de la mise en valeur*. Hayez, Bruxelles, 620 pp .

Spell, T.L., McDougall, I. (2003). Characterization and calibration of $^{40}Ar/^{39}Ar$ dating standards. Chem. Geol., 198, 189 - 211.

Steiger, R.H., Jäger, E. (1977). Subcommission on geochronology: convention on the use of decay constants in geo- and cosmoschronology. Earth and Planetary Science Letters, 36, 359-362.

Tack, L., Fernandez-Alonso, M., Wingate, M., Deblond, A. (1999). Critical assessment of recent unpublished data supporting a single and united geodynamic evolution of the Sao Francisco-Congo-Tanzania cratonic blocks in the Rodinia configuration. Journal of African Earth Sciences, 28, 75–76.

Tembo, F., Kampunzu, A.B., Porada, H. (1999). Tholeiitic magmatism associated with continental rifting in the Lufilian Fold Belt of Zambia. J. Afr. Earth Sci., 28(2), 403-425.

Tembo, F., Kampunzu, A.B., Musonda, B.M. (2000). Geochemical characteristics of Neoproterozoic A-type granites in the Lufilian Belt, Zambia. J. Afr. Earth Sci., 30(4A), p. 85.

Tetley, N., MacDougall, I., Heydegger, H.R. (1980). Thermal neutron interferences in the ^{40}Ar-^{39}Ar dating technique. Journal of Geophysical Research, 85, 7201-7205.

Thieme, J.G. (1971). The Geology of Musonda Falls Area, Explanation of Sheet 1028, SE Quarter. Geological Survey of Zambia, Report No. 32, 25 pp.

Tshileo, P.M., Walisumbu, C.K., Kaluendi, K. (2003). The Kipushi Zn-Pb-Cu deposit. In: Guide-Book to the Field Trip, IGCP No. 450, Proterozoic Sediment-hosted Base Metal Deposits of Western Gondwana; Conference and Field Workshop Lubumbashi 2003, Lubumbashi, D.R. Congo, 210-213.

Vanden Brande, P. (1936). Etudes géologiques dans le feuille Lukafu. Ann. Serv. Mines Comité Spécial du Katanga, 6, 51-69.

Wendorff, M. (2001a). New exploration criteria for 'megabreccia'-hosted Cu-Co deposits in the Katangan belt, central Africa. In: Piestrzynski, A. et al. (Eds.), Mineral Deposits at the Beginning of the 21st Century. Swets & Zeitlinger Publishers, Lisse, Netherlands, pp. 19-22.

Wendorff, M. (2001b). Evolution of the Katangan belt foreland basins: Neoproterozoic-Lower Palaeozoic of Zambia and the Democratic Republic of Congo. Abstract, 21st IAS-Meeting of Sedimentology, 3 - 5 September 2001, Davos, Switzerland.

Wendorff, M. (2002a). Megabreccias of the Katangan orogen (Neoprotero-zoic-Lower Palaeozoic of Central Africa): criteria for re-interpretation as synorogenic conglomerates. 16th International Sedimentological Congress, Abstracts Volume, Rand Afrikaans University, Johannesburg, South Africa, 395-396.

Wendorff, W. (2002b). Synorogenic conglomerates and evolution of foreland basins in the external fold-thrust belt of the Katangan orogen, Neoproterozoic-L. Palaeozoic of Zambia and the Democratic Republic of

Congo. 16th International Sedimentological Congress, Abstracts Volume, Rand Afrikaans University, Johannesburg, South Africa, 397-398.

Wendorff, M. (2003a). Stratigraphy of the Fungurume Group- evolving foreland basin succession in the Lufilian fold-thrust belt, Neoproterozoic-Lower Palaeozoic, Democratic Republic of Congo. South African Journal of Geology, 106, 47-64.

Wendorff, M. (2003b). Conglomerates and sedimentary megabreccia (olistostrome) in Roan-Mwashya succession in Mufulira, Copperbelt of Zambia. In: Contributions presented at the 3rd IGCP-450 Conference, Proterozoic Sediment-hosted Base Metal Deposits of Western Gondwana; Conference and Field Workshop Lubumbashi 2003, Lubumbashi, D.R. Congo, 94-97.